CYTOCHROME P450 SUBSTRATE SPECIFICITIES, SUBSTRATE STRUCTURAL TEMPLATES AND ENZYME ACTIVE SITE GEOMETRIES

David F.V. Lewis[a], Maurice Dickins[b], Peter J. Eddershaw[b], Mike H. Tarbit[b] and Peter S. Goldfarb[a]

[a]*School of Biological Sciences, University of Surrey, Guildford, Surrey, GU2 5XH, UK*
[b]*GlaxoWellcome Research & Development Limited, Park Road, Ware, Hertfordshire, SG12 0DP, UK*

CONTENTS

SUMMARY

The structural characteristics of human cytochrome P450 substrates are outlined in the light of extensive studies on P450 substrate specificity. Templates of superimposed substrates for individual P450 isozymes are shown to fit the corresponding enzyme active sites, where contacts with specific amino acid residues appear to be involved in the interaction with each structural template. Procedures leading to the evaluation of likely P450 specificity, binding affinity and rate of metabolism are described in the context of key examples in which molecular modelling appears to rationalize experimentally observed findings.

1. INTRODUCTION

The important roles of mammalian cytochrome P450 isoforms in the Phase 1 metabolism of drug substrates and other xenobiotics have been well established /1-4/. In particular, there is growing interest in the rationalization of P450-mediated drug metabolism in man /3,4/ where evidence is accumulating for the role of individual P450 isozymes in the clearance of the majority of chemicals in current clinical use /5,6/.

Recently, Smith and colleagues have drawn attention to the status of human P450 models /3/ and to the characteristics of substrates and inhibitors of human P450 isoforms /4/. The purpose of this review article is to build on the work previously expounded by Smith and coworkers /3,4,7,8/ (which has also been explored by others /9,10/) on the structural basis of P450 substrate specificity by demonstrating that there is an emerging pattern exhibited by recent mammalian P450 models which concords satisfactorily with current evidence on P450-mediated metabolism of drug substrates in *Homo sapiens*.

2. SUBSTRATES OF P450 ISOFORMS FROM FAMILIES CYP1, CYP2 AND CYP3

For mammalian microsomal P450s involved in the metabolism of foreign compounds, it is possible to formulate some general characteristics of substrates for certain P450 families and subfamilies, despite the fair degree of structural diversity that is known to exist in the

compounds which are relatively specific for different P450 isoforms. Table 1 summarizes some recent information /5/ on human hepatic P450s and their substrates, inducers and inhibitors, together with the average percentages of the individual P450s in human liver. The general characteristics of the substrates for mammalian P450 isoforms associated with the metabolism of xenobiotics are summarized in Table 2, although it should be appreciated that structurally diverse compounds may, nevertheless, be substrates of the same P450, provided that the criteria for binding to that particular P450 are fulfilled. This could involve, for example, the possession of a hydrogen bond potential at a certain distance relative to an aromatic ring system, such that orientation for metabolism is governed by key interactions with complementary active site residues.

Some of the species differences in metabolism of xenobiotics can be explained on the basis of small but, nevertheless, significant changes in the active site regions of the relevant orthologous P450s. For example, there are differences in the metabolism of coumarin by rat, mouse and human CYP2A orthologues which appear to be rationalized in terms of amino acid residue contacts within the putative substrate binding sites in the P450s concerned /11/. Furthermore, the hepatic complement of P450 isoforms differs within mammalian species, particularly between *Homo sapiens* and experimental animals, such as rat, mouse and rabbit, in which there are alterations in P450 regulation and expression which affect the way in which certain xenobiotics are metabolized. However, as far as the metabolic activation of carcinogens is concerned, it would appear that the same P450 orthologues (namely:- CYP1A1, CYP1A2 and CYP2E1) are involved for both human and experimental rodent species /12-14/, presumably because there are relatively few differences between the orthologous P450 proteins in these cases. This is supported by high sequence homologies between the different mammalian species /12/.

Based on accumulated evidence from physicochemical and structural data, Smith and colleagues formulated a number of general rules for human P450 substrate selectivity /4/. These centre primarily on compound lipophilicity and degree of ionization at physiological pH (i.e. 7.4) such that likely P450 specificity can be governed by substrate partitioning between aqueous and lipid phases. The important quantities in this respect are: log P, pKa and $\log D_{7.4}$, where log P is the logarithm of the n-octanol/water partition coefficient, pKa is the

TABLE 1

Human xenobiotic-metabolizing P450s /5,101-103/

CYP	% hepatic P450	% involvement in drug oxidations	Typical Substrate	Catalyzed reaction	Inhibitor	Inducer
1A1	<1	2.5	7-ethoxyresorufin	O-deethylation	9-hydroxy ellipticine	TCDD
1A2	13	8.2	caffeine	N_3-demethylation	furafylline	heterocyclic amines
1B1	<1	unknown	17β-estradiol	4-hydroxylation	propotol	indolocarbazole
2A6	4	2.5	coumarin	7-hydroxylation	pilocarpine	phenobarbital
2B6	<1	3.4	7-ethoxy-4-trifluoromethyl coumarin	O-deethylation	orphenadrine	phenobarbital
2C9	18	15.8	tolbutamide	4-methyl hydroxylation	sulfaphenazole	barbiturates
2C19	1	8.3	omeprazole	5-methyl hydroxylation	fluconazole	barbiturates
2D6	≤2.5	18.8	debrisoquine	4'-hydroxylation	quinidine	none known
2E1	≤7	4.1	4-nitrophenol	2-hydroxylation	4-methyl pyrazole	ethanol
3A4	≤28	34.1	nifedipine	N-oxidation	ketoconazole	dexamethasone

TCDD = 2,3,7,8-tetrachlorodibenzo-p-dioxin

TABLE 2

Characteristics of mammalian P450 substrates /25/

CYP	Broad classification of specific substates
1A1	Planar polyaromatic hydrocarbons and their derivatives
1A2	Planar polyaromatic/heterocyclic amines and amides
2A	Relatively low molecular weight compounds including ketones and nitrosamines
2B	Non-planar molecules many with V-shaped structures
2C	Relatively non-planar molecules including amides and sulphonamides
2D	Basic compounds with a nitrogen atom protonable at physiological pH
2E	Low molecular weight compounds of diverse structure
3A	High molecular weight compounds of diverse structure

Notes:
1. There is some degree of overlapping substrate specificity for: CYP1A1 and CYP1A2, CYP2A and CYP2E, CYP2B and CYP2C, although certain characteristics such as lipophilicity and hydrogen bond forming potential can provide a means of distinguishing between specific substrates in each category.
2. Phenobarbital and other barbiturates induce P450s of subsfamilies CYP2A, CYP2B, CYP2C and CYP3A, whereas dexamethasone induce both CYP3A and CYP2A. Moreover, TCDD and other polyaromatics induce both CYP1A and CYP2A subfamilies. However, CYP2E is induced by acetone, ethanol and benzene, indicating that there are both similarities and differences in the regulatory mechanisms of mammalian P450s.

negative logarithm of the acid/base dissociation constant, and log $D_{7.4}$ is the logarithm of the distribution coefficient at pH 7.4. The log D value is related /15/ to log P and pKa by the following expressions:-

$$\log D = \log P - \log (1+10^{pH-pKa}) \qquad \text{for weak acids}$$

$$\log D = \log P - \log (1+10^{pKa-pH}) \qquad \text{for weak bases}$$

although these only apply to monoprotic compounds, and more complex expressions are required for diprotic and triprotic substances. Computer programs, such as Prolog P and Prolog D /16/ from CompuDrug Limited, enable the calculation of log P, pKa and log $D_{7.4}$ for compounds for which the experimental values are unavailable, and it has been reported that the degrees of correlation between calculated and experimental log P values are about 0.98 for simple organic compounds /17/. The following subsections describe various physico-chemical characteristics for the major human P450 substrates, indicating how some of these properties are related to active site interactions.

a) CYP2D6

From considerations of the partition coefficients, ionization constants and distribution coefficients of various human P450 substrates, Smith and coworkers have reported, for example, that pKa values for CYP2D6 substrates vary from 7.4 to 12.9 /7/ with log $D_{7.4}$ values of between -3.0 and 1.1 /8/. Although these basic compounds exhibit relatively low lipophilicity due to the effect of ionization at pH 7.4, there is a good correlation between log K_i and log $D_{7.4}$ for a series of β-blockers displaying inhibitory potential against dextromethorphan O-demethylation activity, which is CYP2D6 mediated /4/. Such findings point to the likelihood of hydrophobic interactions between CYP2D6 substrates in terms of their basicity, with sites of metabolism being around 5-7Å from the basic nitrogen, but with some degree of lipophilicity when only the neutral form is considered /4/. There is also the likelihood of hydrogen bond formation at distances from the site of metabolism comparable to those reported for the protonable nitrogen /18/. As shown in the following section, the putative active site of the enzyme appears to have complementary amino acid residues for the binding of the basic, hydrophobic and hydrogen bond donor/acceptor groupings encountered in the majority of CYP2D6 substrates /19/.

b) CYP2C9

In contrast, most CYP2C9 substrates tend to be weakly acidic with pKa values of between 4.5 and 5.9, thus leading to log $D_{7.4}$ values in the octanol/water system ranging from 0.2 to 2.4 which, consequently, exhibit some degree of overlap with those recorded for CYP2D6 substrates /4/. Furthermore, the ionizable acidic function generally lies between 7 and 11Å of the site of metabolism in CYP2C9 substrates /7/. It should be recognized, however, that not all CYP2C9-specific chemicals are weak acids; neither do they all contain a carboxylic acid functional group. Nevertheless, those which possess amide or sulphonamide groupings may become weakly ionizable at physiological pH and, moreover, can enter into hydrogen bonded interactions with donor or acceptor groups within the CYP2C9 active site. The hydrogen bond potential of CYP2C9 substrates can be appreciated by comparing their log $D_{7.4}$ values between octanol/water and cyclohexane/water systems /4/. The use of the hydrocarbon solvent relative to octanol unmasks the hydrogen bond forming properties of CYP2C9 substrates such that their log $D_{7.4}$ values are substantially lower in the cyclohexane system, some of which become negative in value /4/, thus indicating hydrophilic character. It has also been established that the hydrogen bond donor/acceptor atoms in CYP2C9 substrates generally lie between 5 and 7Å from their sites of metabolism by this enzyme /20/, although greater distances have been observed in some instances.

c) CYP3A4

The effect of changing the solvent from octanol to cyclohexane in log P determinations also enables discrimination between CYP2C9 and CYP3A4 substrates /4/, because the difference (Δ log P) is less pronounced in the latter. The inference drawn from these findings is that CYP3A4 substrates are generally more hydrophobic than those of CYP2C9 /4/. In the octanol/water system, the log $D_{7.4}$ values of most CYP3A4 substrates are within the range 0.8 to 8 or more with an average value of around 3 /8/, thus confirming their relatively lipophilic nature coupled with a variable degree of ionization. However, consideration of the molecular structures of a superimposed template of CYP3A4-specific compounds indicates that these also possess a hydrogen bond donor/acceptor site at between 5 and 8Å from their sites of metabolism /21/ despite considerable variations in both

molecular mass (ranging from 288 for testosterone to 1203 for cyclosporin) and chemical structure; although many CYP3A4 substrates are characterized by relatively large-sized molecules compared with the substrates of other P450s /21/. There is, furthermore, some evidence that another potential hydrogen bond donor/acceptor atom is present in a substantial number of CYP3A4 substrates, but at a greater distance from the site of metabolism. In fact, there appear to be two hydrogen bond donor/acceptor amino acid residues within the putative active site of CYP3A4 which correspond to the distance constraints in most substrates /21/.

Smith and coworkers have drawn attention to the hydrophobic character of many CYP3A4 substrates /4/ which indicates that the enzyme active site comprises an essentially lipophilic environment, so one would expect that there are hydrophobic amino acid sidechains lining the haem pocket which may complement groupings on typical CYP3A4 substrates. The following section (§3) will demonstrate that homology modelling of CYP3A4 shows that a substantial number of aromatic and aliphatic hydrophobic residues are present within the putative haem environment of the enzyme which can bind equivalent hydrophobic portions of CYP3A4 substrates /21/. Moreover, the relatively large and open nature of the putative active site of CYP3A4 would explain the fact that some substrates are oxidized at more than one position in the molecule*, as rotation of the structures of substrates (such as cyclosporin and terfenadine) within the CYP3A4 binding site helps to rationalize their CYP3A4-mediated metabolism at different regions of the molecule.

d) CYP2E1

In contrast, substrates of CYP2E1 are characterized as relatively small-sized molecular structures /22/, although their log P or log $D_{7.4}$ values indicate that enzyme-substrate interactions are generally hydrophobic in nature /4/. These neutral, small molecular weight compounds may be either aromatic or aliphatic with log $D_{7.4}$ ranging from -0.3 for ethanol to 2.3 in the case of halothane /4/, and some CYP2E1 substrates have hydrogen bond forming potential relatively close to their sites of metabolism. By and large, the more lipophilic CYP2E1 substrates tend to be either carcinogenic or hepatotoxic, with

*This feature is not exclusively shown by CYP3A4, however.

compound polarity playing an important role in discriminating between toxic and relatively non-toxic chemicals /22/, although frontier orbital energy levels and, in particular, their difference (ΔE) are also differentiating factors especially with regard to dialkyl nitrosamines /22/. Active site modelling of CYP2E1 substrates shows that both hydrophobic and hydrogen-bonded interactions are possible, due to the presence of complementary amino acid residues which, to some extent, explain how typical substrates may become orientated for metabolism at the experimentally observed positions /22/.

e) CYP1A2

As far as CYP1A2 is concerned, its substrates are probably most readily characterized structurally, as a recurrent feature is an aromatic or heterocyclic ring system, which imparts a relatively planar geometry to the molecule /23/. Although such compounds are fairly lipophilic, a generally basic character of many CYP1A2 substrates tends to give rise to somewhat lowered log $D_{7.4}$ values relative to those of CYP1A1, especially for caffeine (log $D_{7.4}$ -0.1) and the inhibitor, enoxacin (log $D_{7.4}$ -2.2). For the compounds tabulated by Smith *et al.* /4/, the range of log $D_{7.4}$ values extends from -2.2 to 3.0, with pKa values varying from 0.6 to 14.0, although the majority are weak bases with pKa values in the region of 8 to 10 /4/.

In addition to the possession of at least one aromatic or heteroaromatic ring, CYP1A2 substrates contain one or more hydrogen bond acceptor atoms, usually coinciding with the common basic group present in many CYP1A2-specific chemicals /4,23/. The aromatic ring system of CYP1A2 substrates appears to enter into π-π stacking interactions with coplanar aromatic amino acid residues in the putative active site of the enzyme /23/, whereas the formation of two hydrogen bonds between donor amino acid sidechains (possibly threonines) and substrate acceptor atoms is a recurring feature of CYP1A2 active site interactions. Consequently, the common structural characteristics of many CYP1A2-specific chemicals are reflected in the disposition of key amino acid residues in the enzyme's binding site region /23/.

f) CYP2C19

With respect to the CYP2C family isozymes, substrates of the polymorphic form CYP2C19 exhibit certain structural differences compared to those of the homologous CYP2C9 /4,24/, although these are not obvious from consideration of their physicochemical properties such as log P or log $D_{7.4}$ /4,20/. However, the general preference for weakly acidic compounds by CYP2C9 is not apparent in CYP2C19, which appears to be able to accept both neutral and basic substrates /4/. CYP2C19-specific chemicals usually contain an aromatic ring system and exhibit the potential for hydrogen bond formation; many CYP2C19 substrates contain two hydrogen bond donor/acceptor atoms that are situated about 5-8Å from the site of metabolism /20/. There is, furthermore, a fairly well-defined distance range between these two hydrogen bond forming atoms of between 3-6Å with an average value of around 4.5Å /20/. Active site modelling of CYP2C19 indicates that two hydrogen bond donor/acceptor amino acid residues are positioned relative to the haem moiety such that the formation of two hydrogen bonds between enzyme and substrate assist in orientation for metabolism at the known positions /20/. Moreover, a phenylanine residue is situated in the putative active site region of CYP2C19 to enable π-π stacking interactions between its phenyl ring and complementary aromatic groups on most CYP2C19 substrates. There is also a non-conservative change, K72E, between CYP2C9 and CYP2C19 which could explain the preference of the former for weakly acidic substrates as these could form ion pairs with Lys72 in CYP2C9, but not in the CYP2C19 binding site because of the change to an oppositely charged glutamate residue (Glu72).

Table 3 summarizes the physicochemical and structural information for substrates of the major human hepatic drug-metabolizing P450s, whereas the key interatomic distances encountered in human and some rodent P450 substrates are presented in Table 4, together with other structural information on chemicals specific for individual P450s present in mammalian liver. These findings provide opportunities for proposing schemes for evaluating the likely P450 specificity of untested compounds which could, for example, involve a decision tree approach. Figure 1 represents one possibility that can be used predictively for the pre-screening of development chemicals, although some form of automation would facilitate analysis of combinatorial libraries.

TABLE 3

Physiochemical characteristics of human liver P450 substrates /3,4,7,8,71/

CYP	Range of Log D_{74} values			Range of pKa values			Type of Compounds
1A2	-2.2	to	3.0	0.6	to	14.0	planar polyaromatic or heterocyclic amines
2C9	0.2	to	2.4 (or more)	4.5	to	8.3	weakly acidic
2C19	-0.5	to	4.5	3.3	to	10.4	neutral and basic
2D6	-3.0	to	1.1	7.4	to	12.9	basic
2E1	-0.3	to	2.3	neutral			low molecular weight (M_r <200)
3A4	0.4	to	8.0 (or more)	6.8	to	8.1	high molecular weight (M_r ~ 280 to 1200)

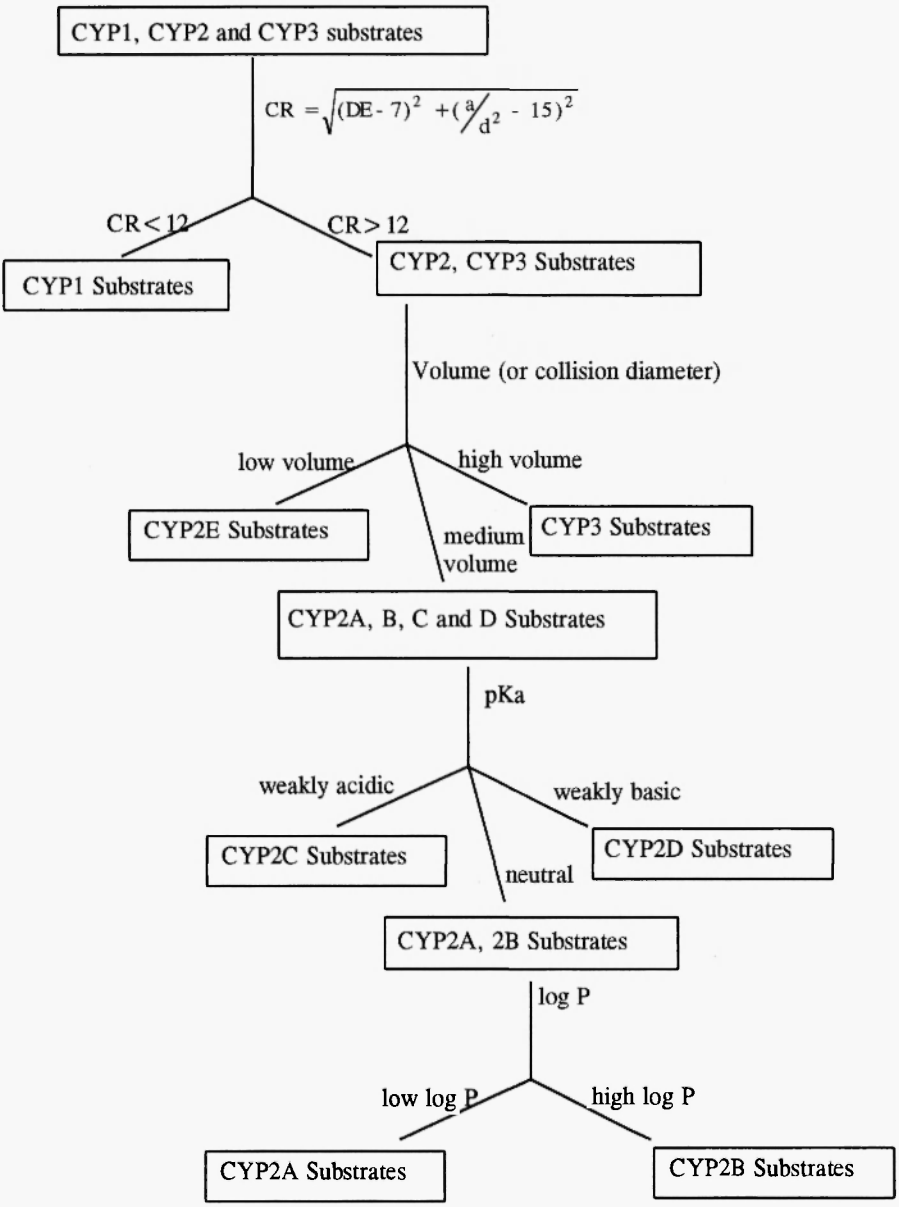

Fig. 1: A proposed Decision Tree Approach for predicting P450 substrate specificity /71,107,109/.

Notes to Figure 1:

1. By and large, the logP values of P450 substrates are greater than zero, although there are exceptions, such as some CYP2D and CYP2E substrates. On average, the log P values of CYP2B substrates (log P ~2.5) are greater than those of CYP2A6 (log P ~1.7).
2. CYP2D6 substrates usually possess a protonatable nitrogen atom 5-7Å from the site of metabolism.
3. CYP2C9 substrates generally possess a hydrogen bond donor/acceptor atom 5-8Å from the site of metabolism.
4. Some compounds can be substrates for more than one P450, especially where there is indication of overlapping specificity from the structural characteristics of the molecules. Moreover, the above scheme does not necessarily apply to steroids and other endogenous chemicals which can be substrates of several P450s.
5. The volume characteristics of P450 substrates facilitates discrimination between CYP3 (average 390Å^3), CYP2E (average 75Å^3) and other CYP2 family enzymes (average 215Å^3).

TABLE 4

Key distances in P450 substrate templates

CYP	Characteristics of most substrates	Reference
1A2	Essentially planar polyaromatic/heterocyclic amines and amides containing one or two hydrogen bond acceptors	Lewis and Lake, 1995 /23/
2A6	Two hydrogen bond donor/acceptors close to site of metabolism	Lewis and Lake, 1995 /11/
2B1	V-shaped molecules with hydrogen bond acceptor around 5-7Å from site of metabolism	Lewis and Lake, 1997 /33/
2C9	Hydrogen bond donor/acceptors 5-7Å from site of metabolism	Lewis et al, 1998 /20/
2C19	Two hydrogen bond donor/acceptors 5-8Å from site of metabolism	Lewis et al, 1998 /20/
2D6	Protonated nitrogen 5-7Å from site of metabolism	Koymans et al, 1992 /104/
2E1	One or two hydrogen bond donor/acceptors close to site of metabolism at 2-4Å and 5-7Å respectively	Lewis et al, 1997 /22/
3A4	Hydrogen bond donor/acceptor 5-8Å from site of metabolism	Lewis et al, 1995 /21/

3. HOMOLOGY MODELS OF HUMAN P450s

The crystal structure of the unique bacterial P450 CYP102 currently represents the preferred template for homology modelling of human and other mammalian microsomal P450s /4,25/. The reasons for this choice lie in the fact that CYP102 exhibits the highest homology of all crystallized bacterial P450s with the mammalian microsomal forms, which may be due to their similarity of redox partner, as an NADPH-dependent FAD- and FMN-containing oxidoreductase flavoprotein is common to the redox systems of both CYP102 and liver microsomal P450s /26/. Since the crystal structure /27/ of the haemoprotein domain of CYP102 has been available, various researchers have produced homology models of microsomal P450s and it has, in many instances, been possible to rationalize the substrate specificity of such modelled P450 isoforms /11,19-23,28-35/.

More recently, the crystal structure of substrate-bound CYP102 has been published /36/ and this may represent an improved starting template for microsomal P450 modelling, particularly as there are clear conformational changes in the haemoprotein which have occurred following substrate binding, such that the derived models of microsomal P450s exhibit closer concordances with experimental information /34/.

Consequently, the P450 models outlined in this work are produced from the substrate-bound CYP102 crystal structure (pdb code: 1fag), and it will be interesting to note any additional changes which may occur following reduction of the substrate-bound haemoprotein, as the structure of this form is currently being determined crystallographically (J.A. Peterson, personal communication). However, movement of substrate towards the haem iron has already been observed spectroscopically via ^{1}H NMR paramagnetic shift measurements /37/ and, therefore, some degree of reorientation of substrate can be assumed once the original position (i.e. that of palmitoleic acid in CYP102) has been used as a guide for the docking of other molecules in P450 homology models. Based on the structures of known P450-substrate complexes, it would appear that the site of metabolism lies between 3 and 4Å from the haem iron. The closest analogy to the dioxygen-bound P450 substrate complex is $P450_{cam}$.CO /38/ in which it is found that the substrate moves almost 1Å away from the haem relative to its position in the initial substrate-bound state /39/. Consequently, one can

utilize these findings to model various stages in the P450 catalytic cycle.

An important prerequisite of any protein homology model, however, is the preparation of a satisfactory amino acid sequence alignment between the crystal structure template and the target protein. Some of the problems encountered using the CYP101 sequence, such as generally low homology and significant gaps in the alignment, have been largely overcome with CYP102 because this form shows higher homology with microsomal P450s with relatively few short gaps in its alignments when compared with CYP101 /25/. Fortunately, sequence alignment between P450s is facilitated by the large body of information reported from site-directed mutagenesis and other experimental studies on specific residues likely to be in contact with substrates or with redox partners, especially for the CYP2 family (reviewed in /34/). Despite reservations expressed regarding the utility of P450 models constructed by homology /39/, it has been found that all of the recent microsomal P450 structures produced from CYP102 are, in fact, highly consistent with experimental observations on substrate specificity /11,19-23,28-35/. In particular, the previously outlined substrate characteristics preferred by individual P450 isoforms can be explained by specific contacts with amino acid residues in the respective P450 active site regions, such that superimposed molecular templates of known P450 substrates will fit satisfactorily within the binding sites of the given human P450 isoforms, including CYP1A2 /23/, CYP2A6 /11/, CYP2B6 /33/, CYP2C9 and CYP2C19 /20/, CYP2D6 /19/, CYP2E1 /22/, CYP3A4 /21/ and CYP4A11 /40/. Some notable examples of these cases will now be discussed, in the light of the newly derived models based on substrate-bound CYP102 /34/. Important contact points in human P450 active sites are shown in Table 5.

4. CYP1A2 ACTIVE SITE INTERACTIONS

The specific marker substrate, caffeine, is N-demethylated in three different positions by human and other mammalian P450s (reviewed in /34/) with the N-3 position representing the preferred site. The preference of CYP1A2 for relatively planar molecules with some hydrogen bond potential is consistent with the putative active site, as shown in Figure 2, which contains caffeine orientated for N_3-

TABLE 5

Important contacts in human P450 active sites*

CYP	SRS1	SRS2	SRS4	SRS5	SRS6
1A2	T115, T124	F226	F319	F384	Y495
2A6	Q104	F209	N296	M365	H477
2B6	1114	F206, S210	S294	L363	E474, C475
2C9	I99, F100	1205	A297	S365	V473, N474
2C19	H99, F100	1205	A297	S365	V473, N474
2D6	T107	E216	D301	V374	F481
2E1	R100	F207	T301, T303	N367	H475
3A4	F102, N104	F213	F304	M371	G479, G480

*=Single letter codes of amino acids are used together with their position in each P450 sequence.
SRS = Substrate recognition site region according to the designation of Gotoh /64/.
Note: It appears that the proposed SRS3 region lies some distance away from the heme pocket and, furthermore, mutagenesis experiments in the area have little effect on substrate binding as reported by Szklarz et al., 1995; Halser et al., 1994 and He, et al., 1994 /46-48/ although it is possible that SRS3 has a role in the surface recognition and access of substrates to the active site.

demethylation. It appears that there are two main hydrogen bond donor residues which can position the caffeine molecule in three possible orientations due to the presence of three hydrogen bond acceptor atoms in caffeine, namely, two carbonyl oxygens and a heterocyclic nitrogen /23/. Two threonine sidechains can donate hydrogen bonds to the two carbonyl oxygen atoms of caffeine which results in the N_3-methyl group being positioned directly above the haem iron such that oxygenation can occur, thus leading to demethylation at this site (see Figure 2). Furthermore, the preference for planar substrates by CYP1A2 can be explained by the presence of two coplanar aromatic residues (phenylalanine and tyrosine) which flank the haem pocket, thus facilitating π-π stacking interactions with complementary substrates /23/. Other aromatic amino acids tend to restrict the size and shape of the CYP1A2 substrate binding site such that only molecules of a certain type can occupy the region. This probably explains the limitations on length and width for relatively planar substrates, whereas hydrogen bond donor residues (including the aforementioned threonines), and their placement with respect to the haem moiety, are able to provide a rationalization for CYP1A2 substrate preferences, such as 7-methoxyresorufin /23/.

Furafylline is a specific inhibitor of CYP1A2 with a marked preference for the human isoform /41/, and it has been shown that the mechanism of inhibition involves hydroxylation at the C_8-methyl group /42/. It is possible to show that furafylline can occupy the putative active site of CYP1A2 in an orientation which presents the C_8-methyl above the haem iron for hydroxylation to occur /23/. Such an orientation involves two hydrogen bond interactions between the same threonines as shown in Figure 2 for caffeine. Although it is difficult to explain the enhanced selectivity of this inhibitor for human CYP1A2 relative to the rat orthologue, it is possible that only one or two key residue changes in the haem environment are responsible for the species difference.

5. CYP2A6 ACTIVE SITE INTERACTIONS

Coumarin 7-hydroxylation is a specific CYP2A6-catalyzed reaction /5/, and Figure 3 shows how this substrate may occupy the putative active site in an orientation which is consistent with the formation of 7-hydroxycoumarin /11/. Complementary amino acid residues flank the

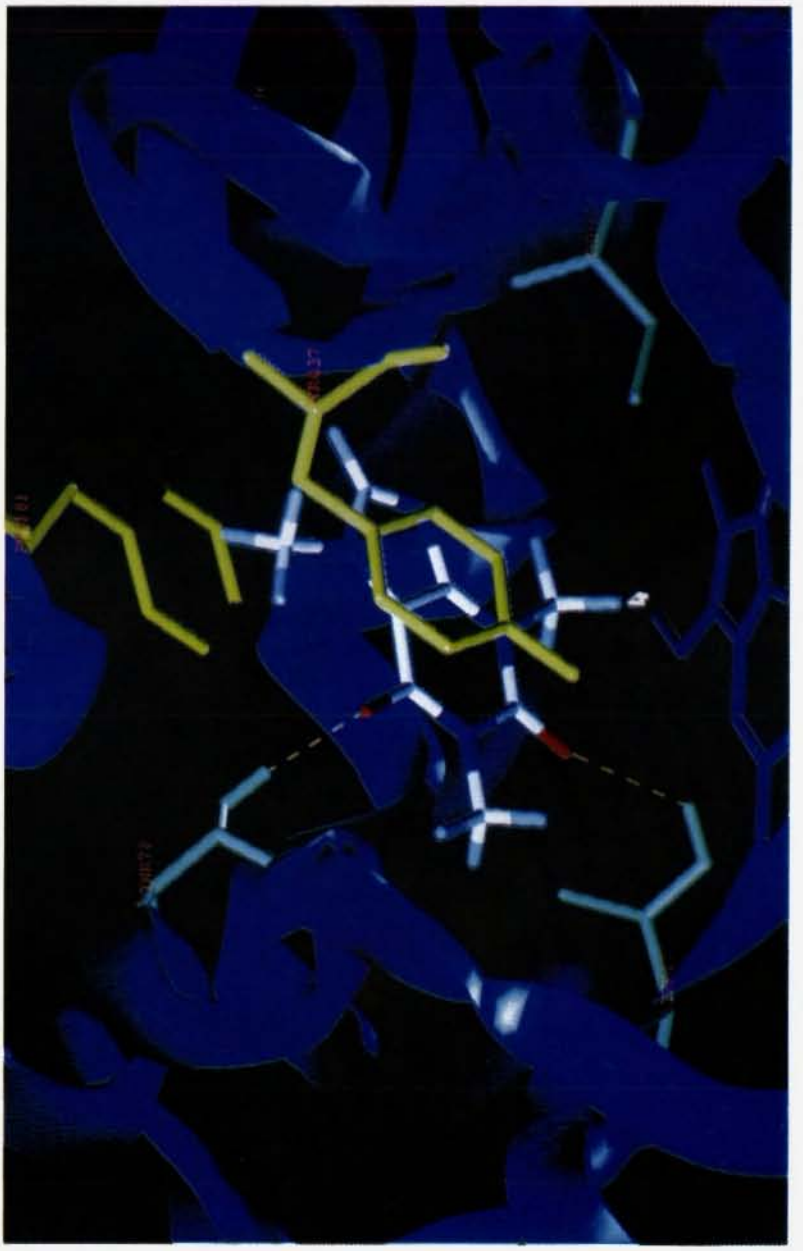

Fig. 2: Putative active site of human CYP1A2 showing the position of caffeine orientated for N_3-demethylation.

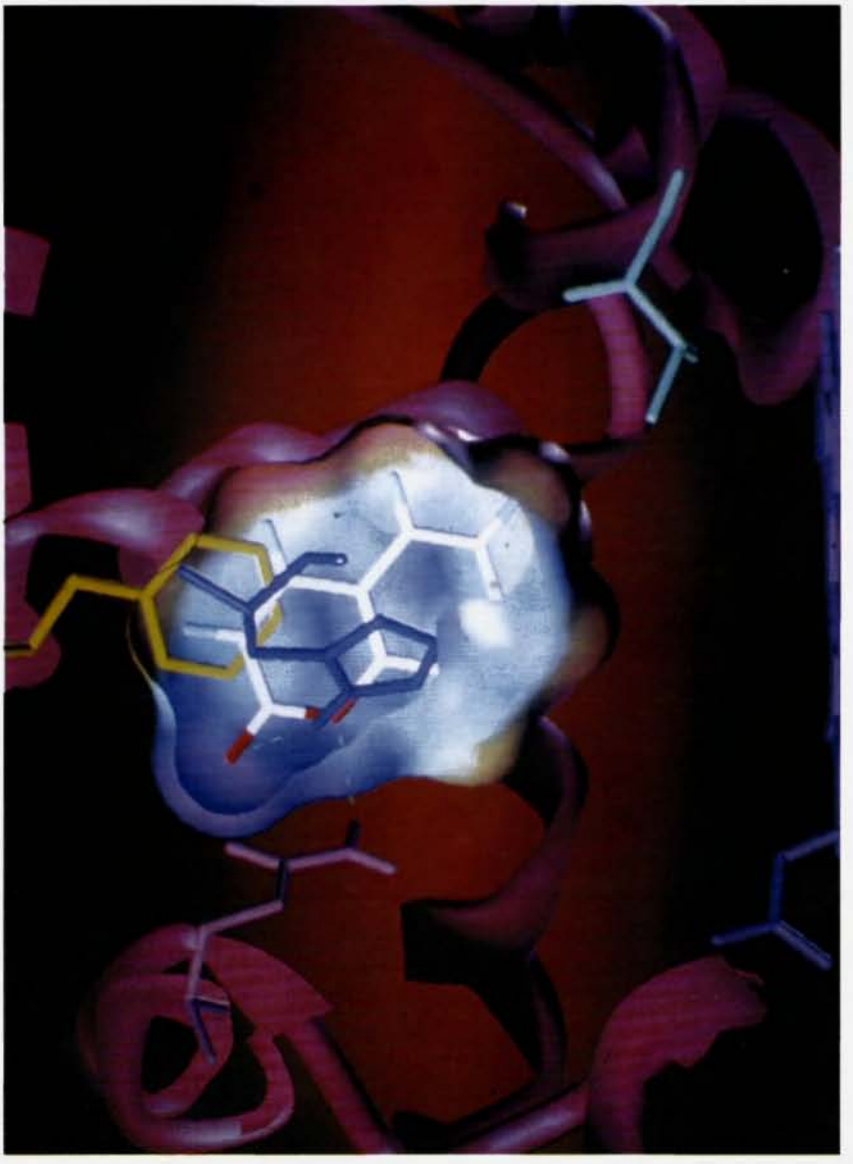

Fig. 3: Putative active site of CYP2A6 with coumarin orientated for 7-hydroxylation.

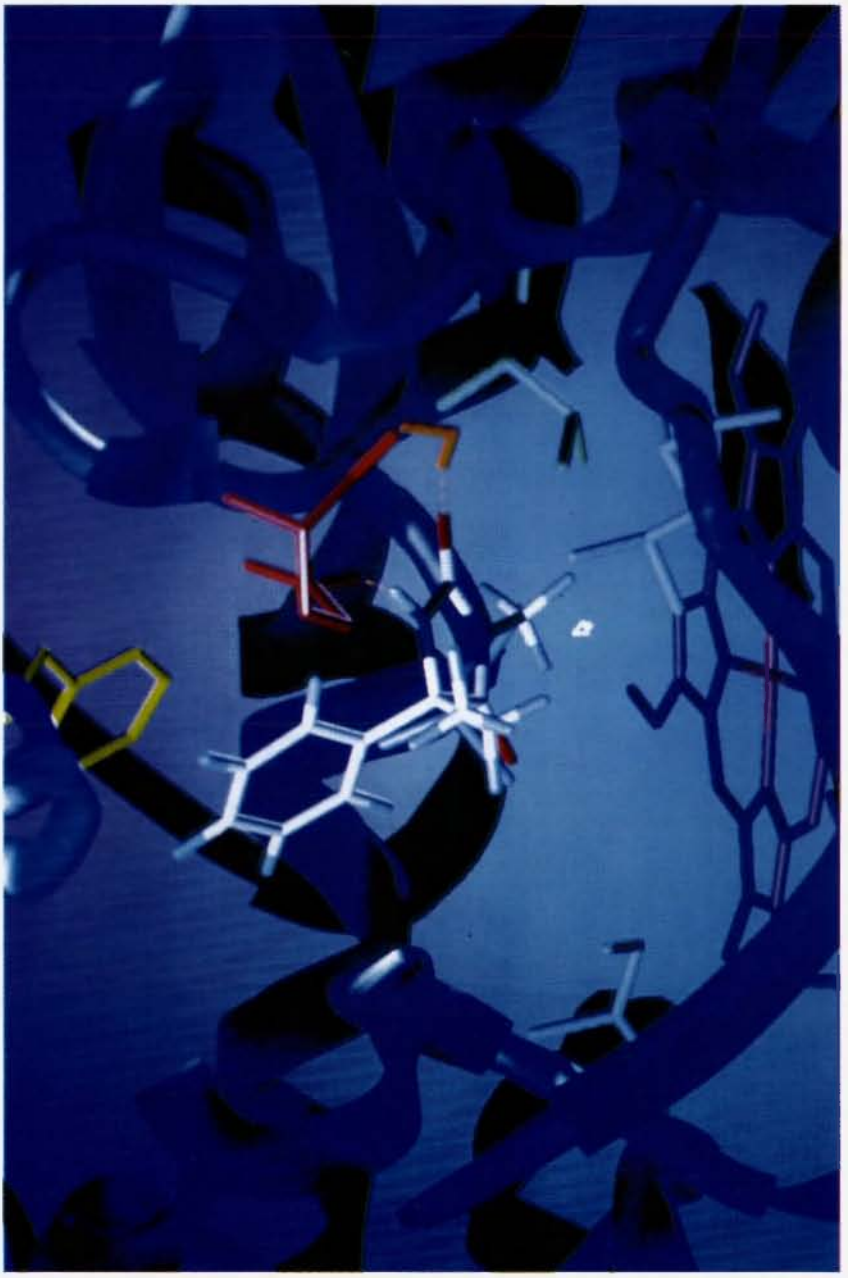

Fig. 4: Putative active site of CYP2B6 showing S-mephenytoin orientated for N-demethylation.

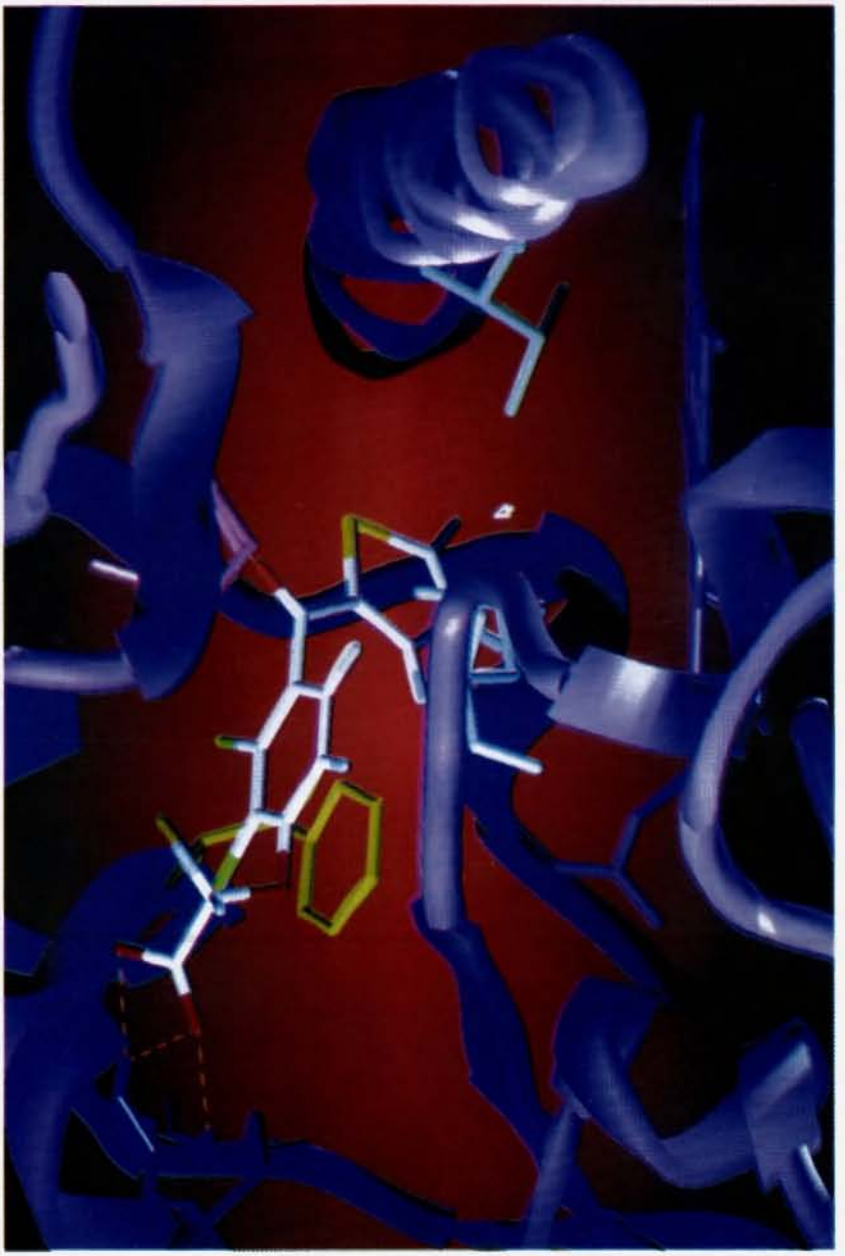

Fig. 5: Puta ive active site of CYP2C9 where tienilic acid is orientated for thiophene ring oxidation

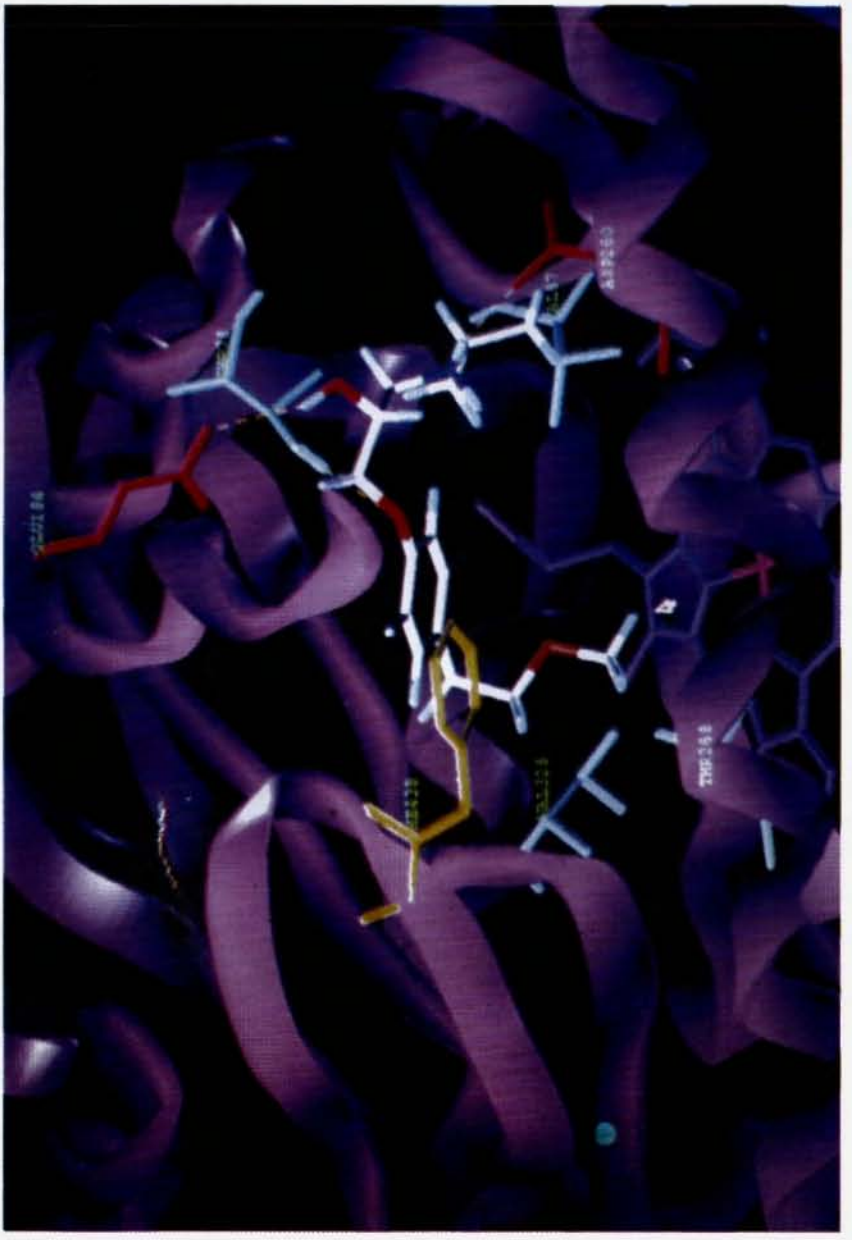

Fig. 6: Putative active site of CYP2D6 with metoprolol positioned for O-demethylation

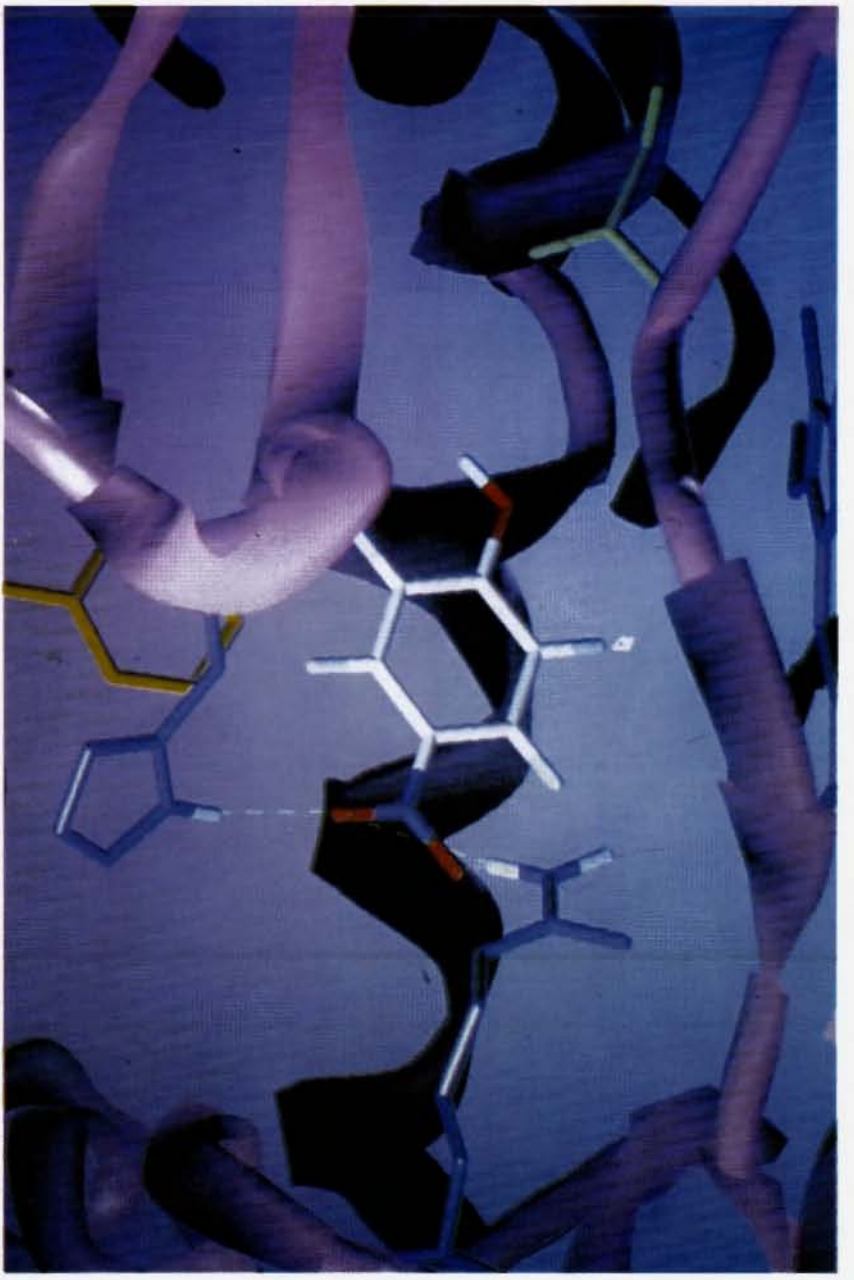

Fig. 7: Putative active site of human CYP2E1 showing p-nitrophenol oriented for 3-hydroxylation

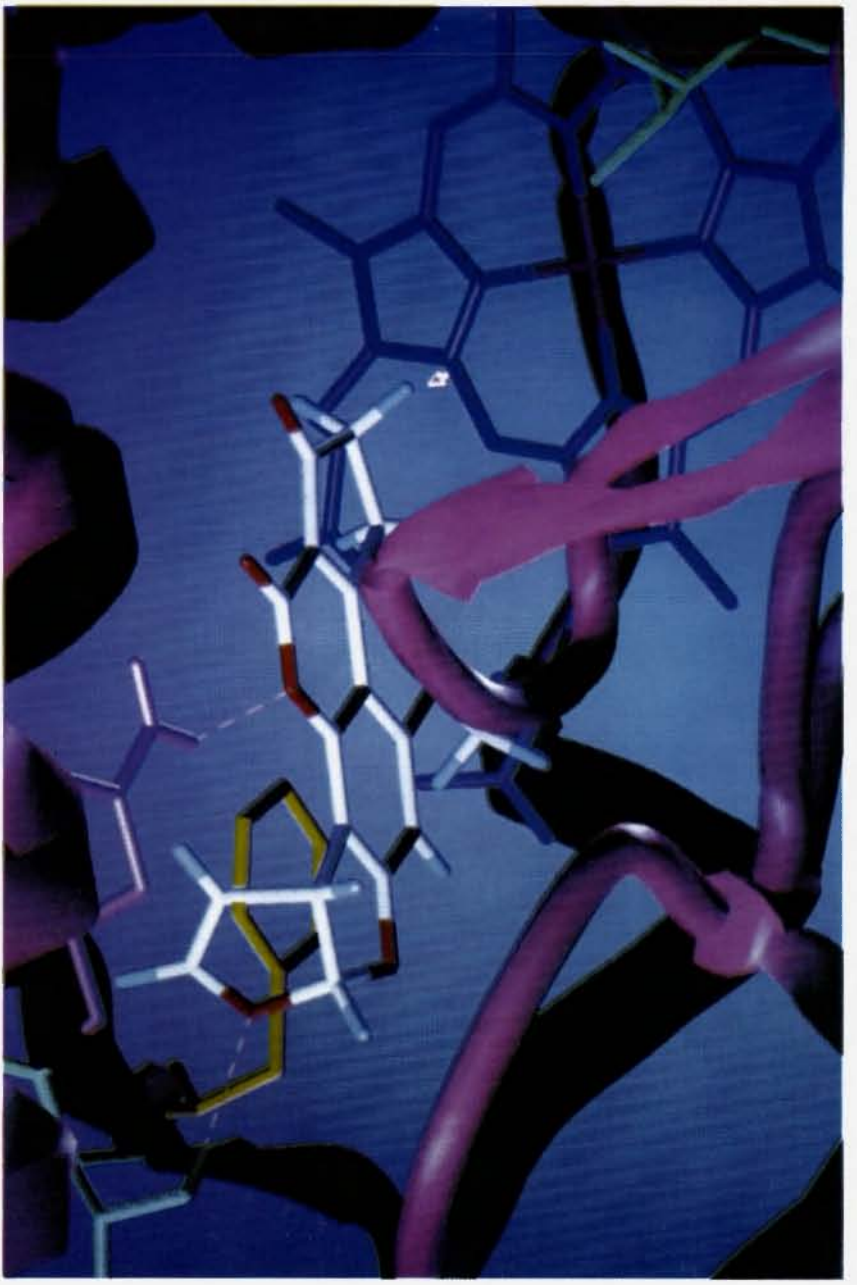

Fig. 8: Putative active site of CYP3A4 where aflatoxin B_1 is positioned for 3α-hydroxylation.

substrate binding site which include Phe181, His437, Gln74 and Arg72; these contact the substrate via intermolecular attractions and position the molecule in such a way that brings the 7-hydrogen directly above the haem iron. In particular, His437 and Gln74 donate hydrogen bonds to the coumarin carbonyl and pyrone oxygen atoms, respectively; whereas Phe181 forms π-π stacking interactions with the aromatic ring system of the substrate. Although present in the putative active site, Arg72 only appears to be involved in binding certain CYP2A6 substrates, with Asn260 representing an additional hydrogen bond donor residue for a relatively small number of known CYP2A6-specific compounds.

Some of the aforementioned residues have been demonstrated, by site-directed mutagenesis in the CYP2A subfamily, to be involved in substrate binding. For example, position 74 corresponds with Gln104 in CYP2A11 that is known to alter substrate regioselectivity; whereas Phe209 in CYP2A5 maps onto position 181 in the alignment, and its change to leucine dramatically affects substrate specificity in CYP2A4 and CYP2A5 /43/. Consequently, there is a satisfactory degree of support from site-specific mutagenesis for the current alignment and the CYP2A6 model derived from it /11/.

6. CYP2B6 ACTIVE SITE INTERACTIONS

In general, CYP2B6 possesses similar substrate specificity /5/ to its more extensively investigated orthologues in experimental mammalian species, namely, CYP2B1 and CYP2B4 /44/. However, certain differences exist and it has been reported /45/ that the N-demethylation of (S)-mephenytoin may represent a drug oxidation specifically metabolized by CYP2B6, although O-deethylation of 7-ethoxy-4-trifluoromethyl coumarin also appears to be CYP2B6-specific /5/. In fact, both of these substrates are able to occupy the putative active site of CYP2B6 in a manner which is consistent with their known routes of metabolism. For example, Figure 4 shows how (S)-mephenytoin may fit the CYP2B6 active site, where complementary interactions with key amino acid residues orientate the molecule such that the N-methyl group is positioned directly above the haem iron. In particular, the phenyl ring of (S)-mephenytoin can form a π-π stacking interaction with the benzene ring of a phenylalanine residue in the F-helix (F206) which has been shown to have a bearing on substrate interactions in the

orthologous rat enzyme CYP2B1 /46/. Furthermore, the ethyl group in (S)-mephenytoin may enter into a hydrophobic interaction with the complementary sidechain of Ile114 (corresponding to Phe87 in CYP102), where the analogous situation in CYP2B1 and CYP2B4 is known to modulate the regioselectivity of steroid metabolism /30,47/. Moreover, the amide NH moiety on the hydantoin ring of (S)-mephenytoin is able to form a hydrogen bond with the acidic sidechain of Glu474, with Cys475 possibly donating a weak hydrogen bond to the amide carbonyl oxygen of the substrate. These energetically favourable interactions orientate the molecule for N-demethylation and can be expected to make contributions to the overall binding affinity, which may be closely related to the apparent K_m value of 564 μM /45/.

Although structurally dissimilar, it is possible to superimpose the molecular structure of the CYP2B6 marker substrate, 7-ethoxy-4-trifluoromethyl coumarin, with that of (S)-mephenytoin in the putative active site of the enzyme where some portions of the specific marker may interact with most of those amino acid residues encountered for (S)-mephenytoin. Additionally, the pyrone carbonyl oxygen of the 7-ethoxy-4-trifluoromethyl coumarin substrate can accept a hydrogen bond from Ser210, which is one position downstream of a mutation site in CYP2B1 /48/. There is also the possibility of a second hydrogen bond being donated from the sidechain of Ser294 to one of the fluorine atoms of the 4-trifluoromethyl group on this substrate. The corresponding residue in CYP2B4 has been shown to be important for androgen regioselectivity /30/, and also Leu363 can form a hydrophobic interaction with the ethyl group of 7-ethoxy-4-trifluoromethyl coumarin. This residue is analogous to a homologous valine in CYP2B1 that is also known to affect androgen regioselectivity /30/. Clearly, therefore, the docking of substrates in the putative active site of CYP2B6 is consistent with both site-specific mutagenesis experiments and CYP2B6-mediated metabolism.

7. CYP2C9 ACTIVE SITE INTERACTIONS

The specific marker substrate for this major human hepatic isoform is tolbutamide, and hydroxylation of its 4-methyl group is CYP2C9-mediated /49/. However, other substrates are known to exhibit lower K_m values towards this isoform, including diclofenac, (S)-warfarin and tienilic acid (reviewed in /20/). Of these, the likely distances between

key atoms on tienilic acid and the haem iron of CYP2C9 have been estimated using NMR spectroscopy /50/, thus providing an opportunity for evaluating the possible residue contacts involved in the binding of this substrate. Figure 5 shows how tienilic acid may interact with amino acid residues within the putative active site of CYP2C9, thus steering the substrate for metabolism on the thiphene ring. The substrate orientation (shown in Figure 5) relative to the haem iron is broadly consistent with reported NMR data on proton paramagnetic shifts /50/, with the suggested cationic site for ion-pairing represented by Arg97. This residue is only two positions upstream of Ile99, which is a known point of contact for substrates binding within the CYP2C9 haem pocket /51/.

Many CYP2C9 substrates contain an acidic grouping which will be ionized at physiological pH /7,20/. Consequently, CYP2C9 substrates, such as tienilic acid, diclofenac and ibuprofen, can be expected to bind via ion-pairing to Arg97 (or to another basic residue) thus determining that the likely site of metabolism will be about 8Å from their ionized carboxylate moiety /52/. Moreover, such electrostatic interactions are likely to make significant contributions to the overall binding affinity and, presumably, therefore explain the relatively low K_m values for these substrates (reviewed in /20/).

In addition to this anionic contact, two hydrogen bond interactions are apparent in the binding orientation of tienilic acid within CYP2C9 (see Figure 5). These are Asn474 and Thr364, each of which donate a hydrogen bond, respectively, to the carbonyl and phenoxy oxygen atoms in the substrate. Furthermore, both of these amino acids are adjacent to mutation sites in CYP2C subfamily enzymes: Asn474 is one position downstream of the residue corresponding to Val473 in CYP2C1, which has a bearing on enzyme activity /53/, whereas Thr364 lies one residue upstream of a serine that is equivalent to Ser364 in CYP2C3, a position known to modulate progesterone regioselectivity /54,55/. The aromatic rings of tienilic acid are in close contact with two hydrophobic sidechains in the putative binding site of CYP2C9 (see Figure 5). In particular, the benzene ring of the substrate could form π-π stacking interactions with Phe100, which is adjacent to the mutagenesis site of Ile99; whereas one edge of the thiophene ring on tienilic acid is orientated near to Val113, a position corresponding to related hydrophobic residues in CYP2C1, CYP2C2 and CYP2C3 that have been shown via site-specific mutagenesis to affect catalytic

activity /55-57/. Consequently, it appears that a combination of key active site interactions is able to explain the known CYP2C9-mediated metabolism of tienilic acid, which is consistent with site-directed mutagenesis experiments and NMR spectroscopic observations. Similarly, the binding orientations of other CYP2C9 substrates can be rationalized, together with explaining some of the differences in substrate specificity for CYP2C9 and CYP2C19 /20/.

8. CYP2D6 ACTIVE SITE INTERACTIONS

Metoprolol is an example of a substrate known to be metabolized specifically by CYP2D6,with regio-selectivity of metabolism for O-demethylation exhibited by the R(+)-enantiomer /28/. In Figure 6, metoprolol is shown fitted within the putative active site of CYP2D6 and orientated for metabolism at the O-methyl group, which is positioned directly over the haem iron. A recurrent feature of CYP2D6 substrates is a basic nitrogen atom, protonated at physiological pH, situated on average between 5 and 7Å from the CYP2D6-mediated site of metabolism, as has been described previously /3,4/.

Moreover, an active site aspartate residue (Asp301) has been identified as representing the most likely anionic partner in an electrostatic interaction with CYP2D6 substrates /58/. Figure 6 shows that metoprolol can be orientated such that ion-pairing between its protonated nitrogen and the carboxylate moiety of Asp301 occurs. Moreover, the substrate's benzene ring π-stacks with the phenyl group of Phe481, which is also thought to be involved in substrate binding based on mutagenesis data /59/. It has also been shown that an active site valine residue (Val374) probably forms a hydrophobic interaction with the methoxyethyl substituent of metoprolol /28/. This amino acid is in close contact with the substrate's 4-substituent according to the docking interaction presented in Figure 6, and is possibly directing the position of the methoxy group relative to the haem iron. Additionally, Val119 at the opposite edge of the CYP2D6 binding site could represent another hydrophobic contact with the substrate; in this case, there is clear complementarity between the isopropyl moiety of metoprolol and the valine sidechain.

Furthermore, hydrogen-bonded interactions between enzyme and substrate may occur via the sidechain of Thr107, although Glu216 could represent an alternative point of contact with CYP2D6

substrates /19/. Threonine-107 is modified in an allelic variant of CYP2D6, in which the change T107I brings about a lowering of catalytic activity /105/. Therefore, the majority of active site interactions between metoprolol and CYP2D6 displayed in Figure 6 have been explored via mutagenesis and, moreover, indicate that they are indeed likely to form contacts with this and other CYP2D6 substrates, thus directing the routes of CYP2D6-mediated metabolism.

9. CYP2E1 ACTIVE SITE INTERACTIONS

The specific marker substrate for human and other mammalian CYP2E1 isozymes is p-nitrophenol /60/, which binds to human CYP2E1 with an apparent K_m of 21 μM /61/. Although 4-methyl pyrazole is regarded as a specific inhibitor for human CYP2E1 /5/, inhibition of p-nitrophenol hydroxylase in rat liver microsomes was achieved preferentially by pyridine, with an apparent K_i of 0.4 μM /62/.

Figure 7 illustrates a possible mode of binding for p-nitrophenol with human CYP2E1 which is consistent with hydroxylation at the 2-position /22/. Interactions between the substrate molecule and putative active site residues include π-π stacking and hydrogen bonding with complementary sidechains which orientate p-nitrophenol such that the 2-position lies directly above the haem iron atom (Figure 7). These binding contacts include π-stacking between the substrate's benzene ring and the corresponding phenyl group of Phe207, a residue position which is analogous to phenylalanines that have been the subject of mutagenesis experiments in the CYP2A and CYP2B subfamilies (reviewed by Lewis /34/ and mentioned above). Additionally, two hydrogen-bonded contacts from putative active site basic residues, Arg100 and His475, appear to 'anchor' the p-nitro group of the phenolic substrate and thus position the site of metabolism over the haem moiety. Both of these amino acids map onto regions of CYP2A and CYP2B subfamily isoforms in which site-specific mutations have been carried out, as outlined above.

Furthermore, the hydroxyl group of p-nitrophenol may hydrogen bond with the conserved distal threonine residue (Thr303 in CYP2E1). This has been mutated in the rabbit orthologue, showing alterations in fatty acid substrate regioselectivity /63/. It is also possible /22/ that other CYP2E1 substrates (such as chlorzoxazone) may form hydrogen bonds with alternative active site residues, such as Thr301 and/or

Asn367, and each of these lie with known substrate recognition sites /64/ which have also been explored by site-directed mutagenesis in the CYP2 family (reviewed in /25/ and /34/). Consequently, a variety of complementary sidechains are available for substrate binding within the putative active site of human CYP2E1, which is also relatively compact and, therefore, may only accept low molecular weight substrates, in agreement with the known substrate specificity of this isozyme /4/.

10. CYP3A4 ACTIVE SITE INTERACTIONS

Although CYP3A4 catalyzes a large number of drug oxidations involving many structurally diverse substrates /5,65/ it can be demonstrated that a relatively small number of key interactions are likely to be involved in binding typical CYP3A4-specific compounds /21/. Figure 8 indicates how aflatoxin B_1 (AFB_1) may become orientated within the putative active site of CYP3A4 such that 3α-hydroxylation may occur, which is the major site of CYP3A4-mediated AFB_1 metabolism /66/. In fact, it is also known that the presence of α-naphthoflavone (αNF) modulates the binding and metabolism of AFB_1 and other CYP3A4 substrates, suggestive of an allosteric effect operating within the haem environment /66/.

Site-directed mutagenesis of a region likely to correspond with the putative F-helix in CYP3A4 has indicated that decreased stimulation by αNF is associated with mutations to alanine of residues Leu210, Leu211 and Phe213 /67/, and molecular modelling of CYP3A4 shows that this stretch of peptide lies directly above the haem pocket /21/. The majority of CYP3A4 substrates appear to bind via hydrogen bond interactions primarily with Asn104, but occasionally with Thr103, depending on the presence and disposition of appropriate hydrogen bond acceptors in the molecule /21/. Although these residues have not been the subject of site-directed mutagenesis in CYP3A4, the region conforms with SRS1 in the CYP2 family and, consequently, has been probed via mutagenesis experiments in several CYP2 isozymes, as mentioned above. Furthermore, a phenylalanine residue (Phe102 in CYP3A4) can enter into π-π stacking interactions with coplanar aromatic rings on most CYP3A4 substrates, including AFB_1. Figure 8 shows that AFB_1 is positioned for 3α-hydroxylation by hydrogen bond formation with the sidechain of Asn104, with Thr103 possibly playing

a secondary role in fixing the substrate orientation. Moreover, the phenyl ring of Phe102 aligns with the aromatic nucleus of AFB_1, thus complementing the aforementioned interactions. Consequently, the putative active site of CYP3A4, which is enlarged by the presence of glycines Gly479 and Gly480 /21/, exhibits a consistency with known substrates and inhibitors, including high molecular weight compounds such as cyclosporin A.

11. ESTIMATION OF SUBSTRATE BINDING AFFINITY

The apparent K_m values obtained from kinetics measurements of P450-mediated reactions provide a reasonable means of evaluating likely substrate binding affinities. Although the enzyme-substrate dissociation constant, K_D, represents a more accurate determination of this quantity, these are rarely reported whereas the K_m data are more common. Consequently, the latter have been employed as determinants of experimental binding affinity for the purposes of comparison with calculated values. Table 6 lists the relevant K_m data for typical substrates of the major human hepatic P450s involved in xenobiotic metabolism, together with the derived experimental binding energy ($\Delta G_{expt.}$) based on the relationship:

$$\Delta G = RT \ln K_m$$

where R is the gas constant (1.9872 $cal.deg^{-1}.mole^{-1}$), T is the absolute temperature and ln K_m is the natural logarithm of the K_m value. In addition, experimental log P values are provided for each substrate in Table 6, except in some cases for which the Prolog P-calculated values are given due to the unavailability of the experimental data. To some extent, the log P value can be used to estimate the desolvation component /68/ of the substrate binding energy based on the equation:

$$\Delta G_{part.} = RT \ln P$$

where R is the gas constant, T is the absolute temperature, and $\Delta G_{part.}$ is the partitioning energy between octanol and water, in the case of log P_{oct}, which represents an analogy to the lipophilic environment encountered within the endoplasmic reticular membrane. Although this type of relationship correlates closely with desolvation energies for hydrophobic molecules, compounds with several polar groupings generally give poor comparisons due to the effect of hydrogen

TABLE 6

Substrate binding affinities to human P450s[a]

CYP	Substrate	K_m[b]	ΔG_{exp}[c]	log P[d]	SA[e]	ΔG_{desol}[f]	ΔG_{elec}[g]	ΔG_{calc}[h]
1A2	Caffeine	018 mM	-5.312	0.01	151.612	-3.790	-1.594	-5.384
2A6	Coumarin	21μM	-8.054	1.39	122.162	-3.054	-4.927	-7.981
2B6	(S)Mephenytoin	564μM	-4.608	0.69[i]	165.968	-4.419	-1.482	-4.543
2C9	Tienilic acid	14μM	-8.036	3.97[i]	217.653	-5.441	-4.031	-8.167
2D6	(R)Metoprolol	46μM	-6.152	1.97[i]	254.372	-6.359	-1.337	-6.505
2E1	4-Nitrophenol	21μM	-6.378	2.91	140.029	-4.501	-2.790	-6.291
3A4	Aflatoxin B_1	43μM	-6.194	2.20[i]	200.324	-5.008	-1.505	-6.513

a All energies are given in $kcalmole^{-1}$ using data from references /28,45,50,52,58,62,66/.
b Experimentally determined apparent K_m values (mM or μM)
c Based on $\Delta G_{expt} = RTlnK_m$
d Experimental log P_{oct} value
e Surface area ($Å^2$) of the solvent-accessible Connolly surface
f $\Delta G_{desol} = -25SA/100$
g Electrostatic component of the interaction energy using Gasteiger-Marsili charges on both enzyme and substrate with dielectric constant of unity
h $\Delta G_{calc} = \Delta G_{desol} + \Delta G_{elec}$
i Calculated value using the Pallas system (CompuDrug Ltd, Budapest)

bonding. Consequently, a potentially improved method of calculating desolvation energies involves the use of solvent-accessible surface areas with the relationship:

$$\Delta G_{desol.} = -25SA/1000$$

where $\Delta G_{desol.}$ is the free energy change due to desolvation, and SA is the Connolly surface area in $Å^2$ /69/. It should be recognized, however, that the 25 factor in the above equation represents an average of several determinations and, moreover, may be an underestimate of the actual value /69/. Nevertheless, the currently accepted hydrophobic factor of 25 appears to give satisfactory results for a wide range of structurally diverse chemicals, including the small number evaluated in this study (Table 6).

Although there are several components to the overall binding energy /70/, some of these are relatively minor and, as far as substrate binding to P450 is concerned, it would appear that the desolvation and electrostatic components constitute the major factors /71/. Consequently, the total calculated binding energy, $\Delta G_{calc.}$, as shown in Table 6, can be approximated by the following expression:

$$\Delta G_{calc.} = \Delta G_{desol.} + \Delta G_{elec.}$$

where $\Delta G_{desol.}$ and $\Delta G_{elec.}$ are the desolvation and electrostatic contributions, respectively, to the total calculated binding energy. It has been found, however, that for relatively large molecules, the loss in translational and rotational energy becomes significant, as seems to be the case for omeprazole binding to CYP2C19 /35/.

In Table 6, the electrostatic component, $\Delta G_{elec.}$, is measured directly from the enzyme-substrate complex based on the employment of Gasteiger-Marsili charges and assuming a local dielectric constant of unity. Clearly, this factor represents an estimate of the actual electrostatic contribution to the binding energy, which would require a more rigorous calculation of the partial atomic charges such as that exhibited under the molecular orbital (MO) formalism. In fact, initial results on the $P450_{cam}$ system indicate that semi-empirical procedures (e.g. AM1 and PM3) for MO calculation are able to provide a more satisfactory estimate for the electrostatic contribution to the enzyme-substrate binding energy, although this also involves certain approximations inherent in the methodology. Nevertheless, the results presented in Table 6 are quite reasonable, considering the assumptions made in this

approach, and therefore seem to be fairly promising for future studies in this area.

12. EVALUATION OF P450-MEDIATED REACTION RATES

In contrast to substrate binding affinity, the rates of P450-catalyzed reactions are somewhat difficult to quantify in theoretical terms. The reason for this lies in the complexity of P450-mediated processes together with many different enzyme systems and potentially thousands of substrates. However, it is thought that the rate-determining step in most P450 reactions is the second reduction which precedes the formation of product following rearrangement of the oxygenated complex (reviewed in /25/ and /72/). Nevertheless, it is the binding of substrate which triggers the entire catalytic cycle of P450, and it can be demonstrated that the rate of reaction is governed by the nature of the substrate itself, especially since many key events in the catalytic sequence are substrate-dependent, including the modulation of spin-state and redox equilibria of the haemoprotein (reviewed in /25/ and /72/). It is helpful, therefore, to summarize the various stages involved in the P450 catalytic cycle and then outline factors likely to be related to overall reaction rates in P450 systems.

First of all, the substrate binds to P450 in its low-spin Fe^{3+} state, which leads to the desolvation of the haem environment such that the iron moves to the high-spin state, and a resulting conformational change in the haemoprotein occurs that may 'prime' the P450 for interaction and reduction by its redox partner /25/. Associated with this substrate-induced modulation of the iron spin-state equilibrium is a lowering of the ferric/ferrous redox potential, which facilitates electron transfer such that reduction of ferric P450 can proceed. Sligar and coworkers have shown that there is direct coupling between these two processes, which is in close agreement with the theoretical treatment of the micro-equilibria involved /73-76/. Moreover, Blanck and colleagues have reported that the rates of N-demethylation mediated by CYP2B isozymes appear to be coupled with both spin and redox equilibria for a series of benzphetamines /77-79/.

Consequently, it appears that the structural characteristics of the substrate determine the rate of metabolism and binding affinity for a given P450 and its redox assembly which, in the case of hepatic microsomal P450 system, involves cytochrome b_5, NADPH-dependent

FAD-FMN oxidoreductase and membrane phospholipid /80/. Once the haem iron of P450 has been reduced to the ferrous state, oxygenation occurs and then a second reduction step takes place which is probably rate-limiting in both microsomal and bacterial systems (reviewed in /25/). The oxygenated complex then rearranges to form the metabolite (together with a water molecule) and returns the enzyme to its resting state, i.e. ferric low-spin.

Due to the fact that the second reduction of P450 is the rate-determining step /81/ in most cases, it can be expected that there is a relationship between redox potential (E^o) and rate of P450-mediated metabolism. Indeed, this appears to be borne out experimentally on the basis of data reported by Guengerich /82/ for hepatic microsomal P450s. Table 7 shows the relevant information for a number of purified rat liver P450s; their iron (Fe^{2+}/Fe^{3+}) redox potentials correlate closely with substrate-free turnover number for NADPH oxidation.

TABLE 7

Rat hepatic P450 redox potentials (substrate-free) and turnover of NADPH oxidation /82/

CYP	E^o (mV)	Turnover (min^{-1})
1A2	-305	61
2A1	-327	47
2B1	-311	56
2C6	-336	22
2C11	-321	32
3A1	-350	18

Based on theoretical considerations, the rate of reduction of P450 can be expressed as follows:-

$$\text{rate} = K_a\, k_{ET}\, [P450]\, [Fpt]$$

where K_a is the binding affinity for flavoprotein reductase (Fpt) and P450 of concentrations shown as the bracketed terms, and k_{ET} is the rate constant for electron transfer between reductase and P450 /80/. Calculations show that the electron transfer rate constant is likely to be

related to the distance between interacting redox centres in the two components in the P450 system /25,72/; whereas the binding affinity may be a consequence of the disposition of surface charges on P450 and its redox partner, and it has been demonstrated that a microsomal-type bacterial P450 like CYP102 possesses a well-defined molecular dipole /83/ which could be relevant to redox interactions.

It is probable that substrate occupancy of the P450 active site ensures a change in redox potential of the haemoprotein by altering the extent of haem exposure to the environment /25/. For a range of different haemoproteins, it has been shown that there is a direct relationship between haem exposure and redox potential /84/ in accordance with the expression:-

$$E^{o} = -14.94\% \text{ exposure} + 343.88$$

where E^{o} is the Fe^{2+}/Fe^{3+} redox potential for seven haemoproteins ranging from +320mV to 20mV, and where the correlation coefficient is 0.96 /25/. Extrapolation of this relationship to the P450 system indicates that substrate binding may reduce the percentage of haem surface area exposed to the environment from 44 to 35% for CYP101 /25/. Assuming that substrate-induced desolvation of the haem pocket is responsible for lowering the P450 redox potential which then facilitates reduction of the haem iron, one might anticipate that volume (or surface area) of the substrate solvent-accessible surface will correlate with rate of metabolism. This is, in fact, found to be the case for P450-mediated hydroxylation of p-substituted toluenes /85/ and the relevant QSAR equation is presented in Table 8. Furthermore, a similar relationship (involving surface area) is shown for the N-demethylation of 2,4-dichlorophenoxy-N-alkyl N-methylethylamines /86/, and this is also listed in Table 8.

It is likely, however, that other factors contribute to P450-mediated rates of metabolism. For example, inclusion of dipole moment improves the correlation between molecular volume and the logarithm of hydroxylation rate for 8 p-substituted toluenes /85/, as shown in Table 8. It should also be noted that the oxygen binding affinity is directly proportional to the Fe^{2+}/Fe^{3+} redox potential in both porphyrins /87/ and haemoproteins /88/, with the cysteine proximal ligand in P450 likely to play a role in both oxygen binding and activation /89/. Consequently, there is the suggestion that the substrate-induced lowering of the Fe^{2+}/Fe^{3+} redox potential in P450 facilitates oxygenation in addition to enabling electron transfer from the redox partner.

TABLE 8

Correlations between physicochemical parameters in P450s and their substrates

No.	Relationship	n	s	R	F
1	Turnover no (min^{-1}) = 0.99 $E^0_{Fe^{2+}/Fe^{3+}}$ (mV) +3605	6	8.44	0.91	18.7
2	Redox potential (mV) = -14.94% heme exposure + 343.88	7	37.36	0.96	47.2
3	Redox potential (mV) = 1.48% high-spin - 312.7	5	28.75	0.999	857.6
4	Redox potential = -0.80 ionization energy - 5.63	6	0.22	0.97	55.3
5	- log ζ_{OH} = 0.608 ionization energy + 4.74	50	0.15	0.97	689.7
6	log k_{cat} = 19.97 - 0.024 ΔH^e - 0.94 ionization energy	8	0.08	0.99	93.0
7	log k_{ca} = 19.03 - 1.22 ionization energy	8	0.17	0.93	35.4
8	log k_{ca} = 12.36 - 1.27 ionization energy	21	0.61	0.81	35.9
9	log k_{ca} = 26.90 - 2.58 ionization energy	6	0.13	0.99	145.2
10	log k_{ca} = 23.24 - 2.43 ionization energy	6	0.09	0.97	70.8
11	log k_e = 0.023 + 0.27 ΔE - 0.02 ΔE^2	26	0.69	0.85	62.0
12	log clearance = 0.64 log D_{74} - 0.98 ionization energy + 9.33	12	0.50	0.91	21.4

n = number of points; s = standard error; R = correlation coefficient; F = variance ratio $[(n-2)R^2/(1-R^2)]$

References to data sources:-

1. Guengerich, 1983 /82/
2. Stellwagen, 1978; Lewis, 1996 /84,25/
3. Sligar *et al.*, 1979; Guengerich, 1983 /73,82/
4. Guengerich and MacDonald, 1984 /93/
5. Sabljic and Gusten 1990 /98/
6. Lewis *et al.*, 1995; 1998; Lewis and Pratt, 1998 /85,71,72/
7. Lewis *et al.* 1995; 1993; Lewis and Pratt, 1998 /85,71,72/
8. Taylor and Xu, 1988; Lewis and Platt, 1998 /97,72/
9. Yin, et al, 1995; Lewis and Pratt, 1998 96,72/
10. Tyrakowska, et al, 1996; Lewis and Pratt, 1998 /95,72/
11. Lewis, 1995 /110/
12. Smith, 1997 /100/

Although there is a direct correlation between substrate-induced modulation of iron spin-state equilibria and redox potential in P450 systems /73,77,90/ which appears to be largely determined by the extent of desolvation of the haem environment (*vide supra*), there is evidence to suggest that the substrate redox potential is also an important factor in determining the rate of P450-mediated metabolism /91,92/ and, in some cases, compound redox potential relates closely with ionization potential /93/. As ionization potential (IP) is a readily calculated quantity via molecular orbital (MO) procedures, one could gain insight into variations in P450 substrate metabolism from the relative magnitude of their MO-calculated ionization potentials. Several examples in the literature clearly demonstrate that ionization potential (or energy of the highest occupied MO) correlates with the logarithm of P450-catalyzed rate of metabolism (reviewed in /72/). In particular for series of anilines /94,95/, toluenes /85/, halothanes /96/ and alkenes /97/, log rate relates with either IP or E(HOMO) values in such a way that indicates an underlying similarity of mechanism; this is because IP represents a measure of molecular nucleophilicity and, therefore, suggests that the active oxygen species is an electrophile in these examples.

The fact that the rate of reaction with hydroxyl radicals correlates with IP for a relatively large number of structurally diverse chemicals /98/ points to the possibility of $OH^{\bullet}$ or a similar electrophilic oxygen species being associated with many P450-mediated oxygenations, although there is also evidence for nucleophilic attack in some cases (reviewed in /72/). Table 8 provides a summary of the various inter-relationships outlined above, and it should be added that plotting rate data against IP for some of the series of compounds mentioned previously shows lines of approximately equivalent slope but with displaced intercepts /71/. Consideration of the theory underlying such reactions can provide some degree of rationalization for these findings, however.

According to the Transition State (TS) theory of reaction kinetics (see, for example, reference /99/) the rate constant, k, for any chemical reaction can be equated with the thermodynamics of the TS-formation process as follows:-

$$k = \frac{RT}{Nh} \exp(\Delta S^{\ddagger} / R) \exp(-\Delta H^{\ddagger} / RT)$$

where R is the gas constant, T is the absolute temperature, N is the Avogadro number, h is Planck's constant, and $\Delta S^{\neq}$ and $\Delta H^{\neq}$ are, respectively, the entropy and enthalpy changes involved in the formation of the transition state.

Taking the logarithm of both sides of the above equation gives:-

$$\ln k = \ln\left(\frac{RT}{Nh}\right) + \frac{\Delta S^{\neq}}{R} - \frac{\Delta H^{\neq}}{RT}$$

where the first term will be constant for a given temperature, but $\Delta S^{\neq}$ and $\Delta H^{\neq}$ will vary depending on the type of reaction and may be obtained from the van't Hoff plot which records the variation in log k at different temperatures. In the case of P450-catalyzed reactions, it is possible that the $\Delta S^{\neq}$ term could be related to the desolvation entropy change which accompanies substrate binding (but also modified by the loss in translational and rotational freedom of the molecule) and, as described previously, this can be estimated from the solvent-accessible surface area or volume of the substrate molecule which may also, in turn, correlate with the log P or log D_{74} value /71/. The final term in the above equation could be related to ionization potential of the substrate and, consequently, would readily explain the frequent correlations between log rate and IP outlined previously. However, it is possible that other electronic structural parameters (e.g. E(LUMO), ΔE^{*}, dipole moment and electron densities) may be at least as important, together with the energy change required for hydrogen abstraction from the substrate because this is generally thought to concord with a transition state intermediate formed in P450 reactions. In this respect, the active oxygen species is presumed to abstract a hydrogen atom from the substrate, and this is followed by a rapid recombination between a resulting hydroxy species and the deprotonated substrate to form the hydroxylated metabolite, according to the general reaction sequence:-

$$RH + [O] \rightarrow R^{\bullet} + OH^{\bullet} \rightarrow ROH$$

where RH represents a typical hydrocarbon substrate, [O] signifies the active oxygen species (possibly a bare oxygen atom) and ROH corresponds with the metabolite formed by the P450 oxygenation reaction.

---

* ΔE = E(LUMO) - E(HOMO)

Yin and coworkers have demonstrated that ΔH values for the hydrogen abstraction reaction in halothane derivatives correlates well with rate of P4502E1-mediated metabolism /96/. However, it can also be shown that inclusion of ionization potentials improves this correlation fairly significantly /96/, and the relevant equations are presented in Table 8.

Finally, it should be recognized that the metabolic clearance of P450 substrates can, under certain conditions /108/, be simplified to a straightforward ratio of catalytic rate and binding affinity, as follows:-

$$CL_{int} = \frac{V_{max}}{K_m}$$

where CL_{int} is the intrinsic clearance, V_{max} is the maximal velocity of the reaction, and K_m is the apparent Michaelis constant representing a measure of the substrate's binding affinity towards the relevant P450 isoform involved.

Taking the logarithm for both sides of the above equation produces a simple linear combination relating log clearance with rate and binding energy of the interaction, namely:-

$$\log CL_{int} = \log V_{max} - \log K_m$$

Therefore, although this is an approximation, the relative clearances of substates within a structurally-related series may be proportional to a linear combination of their compound lipophilicity and ionization potential, assuming that log V_{max} correlates with -IP, and that -log K_m is primarily determined by log P (or log $D_{7.4}$) values, although other structural properties may also be involved. It is interesting to note that, for a combination of two different series of chemicals, log clearances do, in fact, correlate with their log $D_{7.4}$ values and ionization energies. The relevant QSAR equation governing this relationship is shown in Table 8 and utilizes the clearance and log $D_{7.4}$ data reported by Smith /100/.

In conclusion, it would appear that relatively simple expressions may be employed in the assessment of P450-mediated rate of metabolism and binding. However, it is important that some degree of active site modelling is employed, in order to investigate the likely structural factors contributing to binding affinity, and to probe the possible steering of metabolism towards certain positions in the substrate under consideration.

ACKNOWLEDGEMENTS

The financial support of GlaxoWellcome Research & Development Ltd., Merck, Sharp & Dohme Ltd., European Union Biomed 2 Programme and the University of Surrey is gratefully acknowledged by one of us (D.F.V.L.).

REFERENCES

1. Nelson DR, Koymans L, Kamataki T, Stegeman JJ, Feyereisen R, Waxman DJ, Waterman MR, Gotoh O, Coon MJ, Estabrook RW, Gunsalus IC, Nebert DW. P450 superfamily: update on new sequences, gene mapping, accession numbers and nomenclature. Pharmacogenetics 1996; 6: 1-42.
2. Bachmann KA. The cytochrome P450 enzymes of hepatic drug metabolism: how are their activities assessed in vivo, and what is their clinical relevance? Am J Therapeut 1996; 3: 150-171.
3. Smith DA, Ackland MJ, Jones BC. Properties of cytochrome P450 isoenzymes and their substrates Part 1: active site characteristics. Drug Discovery Today 1997; 2: 406-414.
4. Smith DA, Ackland MJ, Jones BC. Properties of cytochrome P450 isoenzymes and their substrates Part 2: properties of cytochrome P450 substrates. Drug Discovery Today 1997; 2: 479-486.
5. Rendic S, Di Carlo FJ. Human cytochrome P450 enzymes: a status report summarizing their reactions, substrates, inducers and inhibitors. Drug Metab Rev 1997; 29: 413-580.
6. Bertz RJ, Granneman GR. Use of in vitro and in vivo data to estimate the likelihood of metabolic pharmacokinetic interactions. Clin Pharmacokinet 1997; 32: 210-258.
7. Smith DA, Jones BC. Speculations on the substrate structure-activity relationship (SSAR) of cytochrome P450 enzymes. Biochem Pharmacol 1992; 44: 2089-2098.
8. Smith DA. Species differences in metabolism and pharmacokinetics: are we close to an understanding? Drug Metab Rev 1991; 23: 355-373.
9. Korzekwa KR, Jones JP. Predicting the cytochrome P450 mediated metabolism of xenobiotics. Pharmacogenetics 1993; 3: 1-18.
10. Negishi M, Iwasaki M, Juvonen RO, Sueyoshi T, Darden TA, Pederson LG. Structural flexibility and functional versatility of cytochrome P450 and rapid evolution. Mutat Res 1996; 350: 43-50.
11. Lewis DFV, Lake BG. Molecular modelling of members of the P4502A subfamily: application to studies of enzyme specificity. Xenobiotica 1995; 25: 585-598.
12. Soucek P, Gut I. Cytochromes P450 in rats: structures, functions, properties and relevant human forms. Xenobiotica 1992; 22: 83-103.

13. Nedelcheva V, Gut I. P450 in the rat and man: methods of investigation, substrate specificities and relevance to cancer. Xenobiotica 1994; 24: 1151-1175.
14. Gonzalez FJ, Gelboin, HV. Role of human cytochromes P450 in the metabolic activation of chemical carcinogens and toxins. Drug Metab Rev 1994; 26: 165-183.
15. Avdeef A. Assessment of distribution-pH profiles. In: Pliska V, Testa B, van de Waterbeemd H, eds. Lipophilicity in Drug Action and Toxicology. Weinheim: VCH, 1996; 109-139.
16. Csizmadia F, Tsantili-Kakoulidou A, Panderi I, Darvas F. Prediction of distribution coefficient from structure 1 Estimation method. J Pharm Sci 1997; 86: 865-871.
17. van de Waterbeemd H, Mannhold R. Lipophilicity descriptors for structure-property correlation studies: overview of experimental and theoretical methods and a benchmark of log P calculations. In: Pliska V, Testa B, van de Waterbeemd H, eds. Lipophilicity in Drug Action and Toxicology. Weinheim: VCH, 1996; 401-418.
18. Strobl GR, von Kruendener S, Stockigt J, Guengerich FP, Wolff T. Development of a pharmacophore for inhibition of human liver cytochrome P450 2D6: molecular modelling and inhibition studies. J Med Chem 1993; 36: 1136-1145.
19. Lewis DFV, Eddershaw PJ, Goldfarb PS, Tarbit MH. Molecular modelling of cytochrome P4502D6 (CYP2D6) based on an alignment with CYP102: structural studies on specific CYP2D6 substrate metabolism. Xenobiotica 1997; 27: 319-340.
20. Lewis DFV, Dickins M, Weaver RL, Eddershaw PJ, Goldfarb PS, Tarbit MH. Molecular modelling of human CYP2C subfamily enzymes CYP2C9 and CYP2C19: rationalization of substrate specificity and site-directed mutagenesis experiments in the CYP2C subfamily. Xenobiotica 1998; 28: 235-268.
21. Lewis DFV, Eddershaw PJ, Goldfarb PS, Tarbit MH. Molecular modelling of CYP3A4 from an alignment with CYP102: identification of key interactions between putative active site residues and CYP3A-specific chemicals. Xenobiotica 1996; 26: 1067-1086.
22. Lewis DFV, Bird MG, Parke DV. Molecular modelling of CYP2E1 enzymes from rat, mouse and man: an explanation for species differences in butadiene metabolism and potential carcinogenicity, and rationalization of CYP2E substrate specificity. Toxicology 1997; 118: 93-113.
23. Lewis DFV, Lake BG. Molecular modelling of CYP1A subfamily members based on an alignment with CYP102: rationalization of CYP1A substrate specificity in terms of active site amino acid residues. Xenobiotica 1996; 26: 723-753.
24. Goldstein JA, de Morais SMF. Biochemistry and molecular biology of the human CYP2C subfamily. Pharmacogenetics 1994; 4: 285-299.
25. Lewis DFV. Cytochromes P450: Structure, Function and Mechanism. London: Taylor & Francis, 1996.

26. Fulco AJ. $P450_{BM-3}$ and other inducible bacterial P450 cytochromes: biochemistry and regulation. Ann Rev Pharmacol Toxicol 1991; 31: 177-203.
27. Ravichandran KG, Boddupalli SS, Hasemann CA, Peterson JA, Deisenhofer J. Crystal structure of hemoprotein domain of $P450_{BM-3}$, a prototype for microsomal P450s. Science 1993; 261: 731-736.
28. Ellis SW, Rowland K, Ackland MJ, Rekka E, Simula AP, Lennard MS, Wilf CR, Tucker GT. Influence of amino acid 374 of cytochrome P-4502D6 (CYP2D6) on the regio- and enantio-selective metabolism of metoprolol. Biochem J 1996; 316: 647-654.
29. Modi S, Gilham DE, Sutcliffe MJ, Lian L-Y, Primrose WU, Wolf CR, Roberts GCK. 1-Methyl-4-phenyl-1,2,3,6-tetrahydropyridine as a substrate of cytochrome P450 2D6: allosteric effects of NADPH-cytochrome P450 reductase. Biochemistry 1997; 36: 4461-4470.
30. Szklarz GD, He Y-Q, Kedzie KM, Halpert JR, Burnett, VL. Elucidation of amino acid residues critical for unique activities of rabbit cytochrome P450 2B5 using hybrid enzymes and reciprocal site-directed mutagenesis with rabbit P4502B4. Arch Biochem Biophys 1996; 327: 308-318.
31. de Groot MJ, Vermeulen NPE, Kramer JD, Van Acker FAA, Donné-Opden Kelder GM. A three-dimensional model for human cytochrome P450 2D6 based on the crystal structures of P450101, P450102 and P450108. Chem Res Toxicol 1996; 9: 1079-1091.
32. Lewis DFV, Lake BG, Parke DV. Molecular orbital-generated QSARs in an homologous series of alkoxyresorufins and studies of their interactive docking with cytochromes P450. Xenobiotica 1995; 25: 1355-1369.
33. Lewis DFV, Lake BG. Molecular modelling of human CYP2B isoforms and their interaction with substrates, inhibitors and redox components. Xenobiotica 1997; 27: 443-487.
34. Lewis DFV. The CYP2 family: models, mutants and interactions. Xenobiotica 1998; 28: 617-661.
35. Lewis DFV, Lake BG. Molecular modelling and quantitative structure-activity (QSAR) studies on the interaction of omeprazole with cytochrome P450 enzymes. Toxiclogy 1998; 125: 31-44.
36. Li H, Poulos TL. The structure of the cytochrome $P450_{BM-3}$ haem domain complexed with the fatty acid substrate, palmitoleic acid. Nature Struct Biol 1997; 4: 140-145.
37. Modi S, Sutcliffe MJ, Primrose WH, Lian L-Y, Roberts GCK. The catalytic mechanism of cytochrome P450 BM3 involves a 6Å movement of the bound substrate on reduction. Nature Struct Biol 1996; 3: 414-417.
38. Raag R, Poulos TL. Crystal structure of the carbon monoxide-substrate-cytochrome $P-450_{cam}$ ternary complex. Biochemistry 1989; 28: 7586-7592.
39. Poulos TL. Modelling of mammalian P450s on the basis of $P450_{cam}$ X-ray structure. Meth Enzymol 1991; 206: 11-30.
40. Lake BG, Lewis DFV. The CYP4 family. In: Ioannides C, ed. Cytochromes P450 - Metabolic and Toxicological Aspects. Boca Raton, FL: CRC Press, 1996; 271-297.

41. Sesardic D, Boobis AR, Murray BP, Murray S, Segura J, de la Torre R, Davies DS. Furafylline is a potent and selective inhibitor of cytochrome P450IA2 in man. Br J Clin Pharmacol 1990; 29: 651-663.
42. Kunze KL, Trager WF. Isoform selective mechanism-based inhibition of human cytochrome P450 1A2 by furafylline. Chem Res Toxicol 1993; 6: 649-656.
43. Lindberg RLP, Negishi M. Alteration of mouse cytochrome $P450_{coh}$ substrate specificity by mutation of a single amino-acid residue. Nature 1989; 339: 632-634.
44. Nims RW, Lubet RA. The CYP2B subfamily, In: Ioannides C, ed. Cytochrome P450 - Metabolic and Toxicological Aspects. Boca Raton, FL: CRC Press, 1996; 135-160.
45. Heyn H, White RB, Stevens, JC. Catalytic role of cytochrome P4502B6 in the N-demethylation of S-mephenytoin. Drug Metab Disposition 1996; 24: 948-954.
46. He Y, Luo Z, Klekotka PA, Burnett VL, Halpert JR. Structural determinants of cytochrome 2B1 specificity: evidence of five substrate recognition sites. Biochemistry 1994; 33: 4419-4424
47. Hasler JA, Harlow GR, Szklarz GD, John GM, Kedzie KM, Burnett VL, He Y-A, Kaminsky LS, Halpert JR. Site-directed mutagenesis of putative substrate recognition sites in cytochrome 2B1: importance of amino acid residues 114, 290 and 363 for substrate specificity. Mol Pharmacol 1994; 46: 338-345.
48. Szklarz GD, He Y-A, Halpert JR. Site-directed mutagenesis as a tool for molecular modelling of cytochrome P4502B1. Biochemistry 1995; 34: 14312-14322.
49. Miners JO, Birkett DJ. Use of tolbutamide as a substrate probe for human hepatic P4502C9. Meth Enzymol 1996; 272: 139-145.
50. Polic-Scaife S, Attias R, Dansette PM, Mansuy D. The substrate binding site of human liver cytochrome P4502C9: An NMR study. Biochemistry 1997; 36: 12672-12682.
51. Ibeanu GC, Ghanayem BI, Linko P, Li L, Pedersen LG, Goldstein JA. Identification of residues 99, 220 and 221 of human cytochrome P4502C19 as key determinants of omeprazole hydroxylase activity. J Biol Chem 1996; 271: 12496-12501.
52. Mancy A, Broto P, Dijols S, Dansette PM, Mansuy D. The substrate binding site of human liver cytochrome P4502C9: An approach using designed tienilic acid derivatives and molecular modelling. Biochemistry 1995; 34: 10365-10375.
53. von Wachenfeldt C, Johnson EF. Structures of eukaryotic cytochrome P450 enzymes, In: Ortiz de Montellano PR, ed. Cytochrome P450. New York: Plenum, 1995; 183-223.
54. Hsu M-H, Griffin KJ, Wang Y, Kemper B, Johnson EF. A single amino acid substitution confers progesterone 6β-hydroxylase activity to rabbit cytochrome P4502C3. J Biol Chem 1993; 268: 6939-6944.

55. Richardson TH, Johnson EF. Alterations of the regiospecificity of progesterone metabolism by the mutagenesis of two key amino acid residues in rabbit cytochrome P4502C3V. J Biol Chem 1994; 269: 23927-23943.
56. Kronbach T, Kemper B, Johnson, EF. A hypervariable region of P450IIC5 confers progesterone 21-hydroxylase activity to P450IIC1. Biochemistry 1991; 30: 6097-6102.
57. Straub P, Johnson EF, Kemper B. Hydrophobic side chain requirements for lauric acid and progesterone hydroxylation at amino acid 113 in cytochrome P4502C2, a potential determinant of substrate specificity. Arch Biochem Biophys 1993; 306: 521-527.
58. Ellis SW, Hayhurst GP, Smith G, Lightfoot T, Wang MMS, Simula AP, Ackland MJ, Sternberg MJE, Lennard MS, Tucker GT, Wolf CR. Evidence that aspartic acid 301 is a critical substrate-contact residue in the active site of cytochrome P4502D6. J Biol Chem 1995; 270: 29055-29058.
59. Hayhurst GP. Analysis of the structure-function relationships of P4502D6 by site-directed mutagenesis. Ph.D. Thesis, 1997; University of Sheffield, UK.
60. Koop DR, Laethem CL, Tierney DJ. The utility of p-nitrophenol hydroxylation in P450IIE1 analysis. Drug Metab Rev 1989; 20; 541-551.
61. Tassaneeyakul W, Veronese ME, Birkett DJ, Gonzalez FJ, Miners JO. Validation of 4-nitrophenol as an in vitro substrate probe for human liver CYP2E1 using cDNA expression and microsomal kinetic techniques. Biochem Pharmacol 1993; 46: 1975-1981.
62. Hargreaves MB, Jones BC, Smith DA, Gerscher A. Inhibition of p-nitrophenol hydroxylase in rat liver microsomes by small aromatic and heterocyclic molecules. Drug Metab Disposition 1994; 22: 806-810.
63. Fukuda T, Imai Y, Komori M, Nakamura M, Kusunose E, Satouchi K, Kusunose M. Replacement of Thr-303 of P4502E1 with serine modifies the regioselectivity of its fatty acid hydroxylase activity. J Biochem 1993; 113: 7-12.
64. Gotoh O. Substrate recognition sites in cytochrome P450 family 2 (CYP2) proteins inferred from comparative analyses of amino acid and coding nucleotide sequences. J Biol Chem 1992; 267: 83-90.
65. Li AP, Kaminski DL, Rasmussen A. Substrates of human hepatic cytochrome P4503A4. Toxicology 1995; 104: 1-8.
66. Ueng Y-F, Kuwabara T, Chun Y-J, Guengerich FP. Cooperativity in oxidations catalyzed by cytochrome P4503A4. Biochemistry 1997; 36: 370-381.
67. Harlow GR, Halpert JR. Alanine-scanning mutagenesis of a putative substrate recognition site in human cytochrome P4503A4. J Biol Chem 1997; 272: 5396-5402.
68. Simon Z, Motoc I, Chiriac A. Molecular basis of receptor ligand interactions. In: Voiculetz N, Motoc I ,Simon Z, eds. Specific Interactions and Biological Recognition Processes. Boca Raton, FL: CRC Press, 1993; 17-79.
69. Sharp KA, Nicholls A, Fine RF, Honig B. Reconciling the magnitude of the microscopic and macroscopic hydrophobic effects. Science 1991; 252: 106-109.

70. Williams DH, Searle MS, MacKay JP, Gerhard U, Maplestone RA. Toward an estimation of binding constants in aqueous solution: studies of associations of vancomycin group antibiotics. Proc Natl Acad Sci USA 1983; 90: 1172-1178.
71. Lewis DFV, Eddershaw PJ, Dickins M, Tarbit MH, Goldfarb PS. Structural determinants of cytochrome P450 substrate specificity, binding affinity and catalytic rate. Chem-Biol Inter 1998; 30: 709-737.
72. Lewis DFV, Pratt M. The P450 catalytic cycle and oxygenation mechanism. Drug Metab Rev 1998; 30: 739-786.
73. Sligar SG, Cinti DL, Gibson GG, Schenkman JB. Spin state control of the hepatic cytochrome P450 redox potential. Biochem Biophys Res Comm 1979; 90: 925-932.
74. Sligar SG, Gunsalus IC. A thermodynamic model of regulation: modulation of redox equilibria in camphor monooxygenase. Proc Natl Acad Sci USA 1976; 73: 1078-108.
75. Sligar SG, Gunsalus IC. Proton coupling in the cytochrome P450 spin and redox equilibria. Biochemistry 1979; 18: 2290-2295.
76. Sligar SG. Coupling of spin, substrate and redox equilibria in cytochrome P450. Biochemistry 1976; 15: 5399-5406.
77. Blanck J, Rein H, Sommer M, Ristau O, Smettan G, Ruckpaul K. Correlations between spin equilibrium shift, reduction rate and N-demethylation activity in liver microsomal cytochrome P450 and a series of benzphetamine analogues as substrates. Biochem Pharmacol 1983; 32: 1683-1688.
78. Schwarze W, Blanck J, Ristau O, Janig GR, Pommerening K, Rein H, Ruckpaul K. Spin state control of cytochrome P-450 reduction and catalytic activity in a reconstituted P-450 LM2 system as induced by a series of benzphetamine analogues. Chem-Biol Inter 1985; 54: 127-141.
79. Petzold DR, Rein H, Schwarz D, Sommer S, Ruckpaul K. Relation between the structure of benzphetamine analogues and their binding properties to cytochrome P450LM2. Biochim Biophys Acta 1985; 829: 253-261.
80. Archakov AI, Bachmanova GI. Cytochrome P-450 and Active Oxygen. London: Taylor & Francis, 1990.
81. Imai Y, Sato R, Iyanagi, T. Rate-limiting step in the reconstituted microsomal drug hydroxylase system. J Biochem 1997; 82: 1237-1246.
82. Guengerich FP. Oxidation-reduction properties of rat liver cytochromes P450 and NADPH-cytochrome P450 reductase related to catalysis in reconstituted systems. Biochemistry 1983; 22: 2811-2820.
83. Hasemann CA, Kurumbail RG, Boddupalli SS, Peterson JA, Deisenhofer J. Structure and function of cytochromes P450: a comparative analysis of three crystal structures. Structure 1995; 3: 41-62.
84. Stellwagen E. Haem exposure as the determinate of oxidation-reduction potential haem proteins. Nature 1978; 275: 73-74.
85. Lewis DFV, Ioannides C, Parke DV. A quantitative structure-activity relationship study on a series of 10 para-substituted toluenes binding to

P4502B4 (CYP2B4) and also their hydroxylation rates. Biochem Pharmacol 1995; 50: 619-625.
86. Roffey SJ. Structure-activity relationships in the metabolism of a series of tertiary amines by cytochrome P450. Ph.D. Thesis, 1993; University of Surrey, Guildford, Surrey, UK.
87. Carter MJ, Engelhardt LM, Rillema DP, Basolo F. Oxygen carrier and redox properties of some cobalt chelates including vitamin b_{12}. Chem Comm 1973; 810-812.
88. Addison AW, Burman S. Ligand-dependent redox chemistry of *Glycera dibranchiata* hemoglobin. Biochim Biophys Acta 1985; 828: 362-368.
89. Hawkins BK, Dawson JH. Oxygen activation by heme-containing monoxygenases: cytochrome P450 and secondary amino mono-oxygenase. Active site structures and mechanisms of action. Front Biotransform 1992; 7: 216-278.
90. Blanck J, Ristau O, Zhukov AA, Archakov AI, Rein H, Ruckpaul K. Cytochrome P450 spin state and leakiness of the mono oxygenase pathway. Xenobiotica 1991; 21: 121-135.
91. Watanabe Y, Iyanagi T, Oae S. One electron transfer mechanism in the enzymatic oxygenation of sulfoxide to sulfone promoted by a reconstituted system with purified cytochrome P450. Tetrahedron Lett 1982; 23: 533-536.
92. MacDonald TL, Gutheim WG, Martin RB, Guengerich FP. Oxidation of substituted N_1N-dimthylanilines by cytochrome P450: estimation of the effective oxidation-reduction potential of cytochrome P450. Biochemistry 1989; 28: 2071-2077.
93. Guengerich FP, MacDonald TL. Chemical mechanisms of catalysis by cytochromes P450: a unified view. Accounts Chem Res 1984; 17: 9-16.
94. Cnubben NHP, Vervoort J, Veeger C, Rietjens IMCM. Study of the regioselectivity and mechanism of the aromatic hydroxylation of monofluoroanilines. Chem-Biol Inter 1992; 85: 151-172.
95. Tyrakowska B, Cnubben NHP, Soffers AEMF, Wobbes T, Rietiens IMCM. Comparative MO-QSAR studies in various species including man. Chem-Biol Inter 1996; 100: 187-201.
96. Yin H, Anders MW, Korzekwa KR, Higgins L, Thummel KE, Kharasch ED, Jones JP. Designing safer chemicals: predicting the rates of metabolism of halogenated alkanes. Proc Natl Acad Sci USA 1995; 92: 11076-11080.
97. Traylor TG, Xu F. Model reactions related to cytochrome P450 Effects of alkene structure on the rates of epoxide formation. J Am Chem Soc 1998; 110: 1953-1958.
98. Sabljic A, Gusten H. Predicting the night-time NO_3 radical reactivity in the troposphere. Atmos Environ 1990; 24A: 73-78.
99. Plant AL, Pownall HJ, Smith LC. Transfer of polycyclic aromatic hydrocarbons between model membranes: relation to carcinogenicity. Chem-Biol Inter 1983; 44: 237-246.
100. Smith DA. Physicochemical properties in drug metabolism and pharmacokinetics. In: van de Waterbeemd H, Testa B, Folkers G, eds.

Computer-Assisted Lead Finding and Optimization. New York: Wiley, 1997; 267-276.
101. Guengerich FP. Human cytochrome P450 enzymes. In: Ortiz de Montellano PR, ed. Cytochrome P450. New York: Plenum, 1995; 473-535.
102. Vermeulen NPE. Role of metabolism in chemical toxicity. In: Ioannides C, ed. Cytochromes P450 - Metabolic and Toxicological Aspects. Boca Raton, FL: CRC Press, 1996; 29-53.
103. Honkakoshi P, Negishi M. The structure, function and regulation of cytochrome P4502A enzymes. Drug Metab Rev 1997; 29: 977-996.
104. Koymans L, Vermeulen NPE, Van Acker SABE, te Koppele JM, Heykants JJP, Lavrijsch K, Meuldermans W, Donné-op den Kelder GM. A predictive model for substrates of cytochrome P450-debrisoquine (2D6). Chem Res Toxicol 1992; 5: 211-219.
105. Daly AK, Brockmoller J, Broly F, Eichelbaum M, Evans WE, Gonzalez FJ, Huang J-D, Idle JR, Ingelman-Sundberg M, Ishizaki T, Jacqz-Aigrain E, Meyer UA, Nebert DW, Steen VM, Wolf CR, Zanger VM. Nomenclature for human CYP2D6 alleles. Pharmacogenetics 1996; 6: 193-201.
106. Tassaneeyakul W, Mohamed Z, Birkett DJ, McManus ME, Veronese ME, Tukey RH, Quattrochi LC, Gonzalez FJ, Miners JO. Caffeine as a probe for human cytochromes P450: validation using cDNA-expression, immuno-inhibition and microsomal kinetic and inhibitor techniques. Pharmacogenetics 1992; 2: 173-183.
107. Lewis DFV, Ioannides C, Parke DV. An improved and updated version of the COMPACT procedure for the valuation of P450-mediated chemical activation. Drug Metab Rev 1998; 30: 709-737.
108. Houston JB, Carlile DJ. Prediction of hepatic clearance from microsomes, hepatocytes and liver slices. Drug Metab Rev 1997; 29: 891-922.
109. Lewis DFV, Moereels H, Lake BG, Ioannides C, Parke DV. Molecular modelling of enzymes and receptors involved in carcinogenesis: QSARs and COMPACT-3D. Drug Metab Rev 1994; 26: 261-285.
110. Lewis DFV. COMPACT and the importance of frontier orbitals in toxicity mediated by the cytochrome P450 mono-oxygenase system. Toxicol Modelling 1995; 1: 85-97.